Spontaneous magnetization of an ideal ferromagnet: Beyond Dyson's analysis

Christoph P. Hofmann

Facultad de Ciencias, Universidad de Colima, Bernal Díaz del Castillo 340, Colima C.P. 28045, Mexico

(Received 4 April 2011; revised manuscript received 23 May 2011; published 19 August 2011)

Using the low-energy effective field theory for magnons, we systematically evaluate the partition function of the O(3) ferromagnet up to three loops. Dyson, in his pioneering microscopic analysis of the Heisenberg model, showed that the spin-wave interaction starts manifesting itself in the low-temperature expansion of the spontaneous magnetization of an ideal ferromagnet only at order T^4. Although several authors tried to go beyond Dyson's result, to the best of our knowledge, a fully systematic and rigorous investigation of higher-order terms induced by the spin-wave interaction has never been achieved. As we demonstrate in the present paper, it is straightforward to evaluate the partition function of an ideal ferromagnet beyond Dyson's analysis, using effective Lagrangian techniques. In particular, we show that the next-to-leading contribution to the spontaneous magnetization resulting from the spin-wave interaction already sets in at order $T^{9/2}$—in contrast to all claims that have appeared before in the literature. Remarkably, the corresponding coefficient is completely determined by the leading-order effective Lagrangian and is thus independent of the anisotropies of the cubic lattice. We also consider even higher-order corrections and thereby solve—once and for all—the question of how the spin-wave interaction in an ideal ferromagnet manifests itself in the spontaneous magnetization beyond the Dyson term.

DOI: 10.1103/PhysRevB.84.064414 PACS number(s): 75.40.Cx, 12.39.Fe, 75.30.Ds, 11.10.Wx

I. INTRODUCTION

In a landmark paper on the description of ferromagnets at low temperatures,[1] Bloch introduced the concept of spin waves and identified them as the relevant low-energy degrees of freedom. As an immediate application, he evaluated the leading coefficient in the low-temperature expansion of the spontaneous magnetization: this term, corresponding to noninteracting magnons, is of order $T^{3/2}$. As is well-known, various authors subsequently tried to find the leading term in this series originating from the spin-wave interaction, ending up with conflicting results: corrections to Bloch's law both of order $T^{7/4}$ and T^2 were found.[2–5] The situation remained rather unclear until Dyson, in his pioneering analysis of the thermodynamic behavior of an ideal ferromagnet,[6] showed that the previous results were wrong altogether and that the spin-wave interaction in the spontaneous magnetization starts manifesting itself only at order T^4.

Dyson's motivation was the apparent contradiction between the various results published in the literature. He successfully solved this paradox by setting up a fairly complicated mathematical machinery—in his own words[6]: "The method of the present paper settled the disagreement by showing that both calculations were wrong." In fact, as Dyson states in Ref. 6, a third calculation existed that was also in contradiction with the other two.

Within the past few decades, several articles have appeared dealing with the structure of the series for the spontaneous magnetization *beyond* the Dyson term. Various authors, using different methods, have given their account on what the temperature power of the next-to-leading order term due to the spin-wave interaction should be and how the general structure of the series beyond Dyson should look like. Not all of these results that have appeared in the literature over time, however, as we discuss in more detail later on, are consistent with one another. Our main motivation is thus reminiscent of Dyson's, namely, to determine which one of these calculations yields the correct low-temperature expansion for the spontaneous magnetization of an ideal ferromagnet.

Due to its mathematical rigor, Dyson's calculation is not easy to understand and the perturbative scheme developed for the evaluation of the partition function is fairly complicated. Indeed, after Dyson's analysis, many authors tried to reproduce and rederive his result with alternative methods in a more accessible manner.[7–17] Among these references we would like to point out the paper by Zittartz,[11] about which Dyson comments, "Zittartz replaced my cumbersome mathematics by a simple and elegant construction."[18]

Dyson's analysis and the present work are restricted to the low-temperature regime of the ferromagnet. After Dyson's publication, many articles appeared dealing with the problem of describing the thermodynamic properties of ferromagnets in the *whole* temperature range, i.e., at low temperatures, around the critical temperature T_c, and at high temperatures.[19–37] While these investigations, based on a variety of approaches and methods, correctly reproduced the terms originating from noninteracting magnons at low temperatures, a spurious term of order T^3 appeared in the low-temperature expansion of the ferromagnet. The occurrence of this term is related to what Dyson called the *kinematical* interaction.

Now the kinematical interaction arises due to the transition from physical spin waves to ideal spin waves, which obey Bose statistics—details can be found in Ref. 6. It is this kinematical interaction that complicates the analysis considerably. While the effect of the kinematical interaction is negligible at low temperatures, it becomes crucial as the temperature increases. In particular, the origin of the spurious term of order T^3 in the spontaneous magnetization was readily identified by the authors of the articles cited above: it emerges due to an improper treatment of the kinematical interaction by the Green's function decoupling method or by the random phase approximation theory. On may say that the spurious term of order T^3 was the price one had to pay for formulating an approximate theory attempted to describe the thermodynamics of the ferromagnet in the whole temperature range.

While all these studies were performed within the framework of microscopic or phenomenological theories based on

the Heisenberg model, in the present work, we will follow another approach which has the virtue of being completely systematic and model-independent: the method of effective Lagrangians. Within the effective Lagrangian framework, the structure of the low-temperature expansion of the spontaneous magnetization was analyzed in Ref. 38 up to order T^4 and Dyson's series was reproduced in a straightforward manner. In the effective language, as we will see, this corresponds to including Feynman diagrams for the partition function up to two loops. The effective analysis also readily demonstrated that there is no interaction term of order T^3 in the low-temperature series of the spontaneous magnetization.

In the present work, we go beyond Dyson's analysis and explicitly calculate the effect of the spin-wave interaction beyond T^4 in the spontaneous magnetization of an ideal ferromagnet. To the best of our knowledge, this is the first time that the structure of this power series is given in a fully systematic and rigorous way. Going beyond Dyson's analysis then means that, in the effective Lagrangian framework, we have to consider Feynman diagrams up to three-loop order in the perturbative expansion of the partition function. As it turns out, in the spontaneous magnetization of an ideal ferromagnet, the next-to-leading interaction term already sets in at order $T^{9/2}$—remarkably, the corresponding coefficient is completely determined by the two low-energy coupling constants of the leading-order effective Lagrangian $\mathcal{L}^2_{\text{eff}}$. It does not involve any higher-order effective constants from $\mathcal{L}^4_{\text{eff}}$ where the anisotropies of the cubic lattice start showing up.

Although several authors have also discussed the structure of temperature powers beyond the T^4 term, their conclusions are in contradiction with the systematic effective field-theory approach and therefore erroneous. In particular, to the best of our knowledge, none of the existing calculations ended up with an *interaction* term of order $T^{9/2}$, which in fact represents the leading correction to Dyson's result.

Within the effective Lagrangian framework, we then analyze the general structure of even higher-order corrections in the spontaneous magnetization originating from the spin-wave interaction and show that these are of order $T^5, T^{11/2}, T^6, \ldots$—again contradicting earlier calculations that have appeared in the literature.

The effective Lagrangian method is based on an analysis of the symmetry properties of the underlying theory, i.e., the Heisenberg model in our case, and can universally be applied to systems with a spontaneously broken symmetry. It is formulated in terms of Goldstone boson fields, which represent the dominant low-energy degrees of freedom. The effective Lagrangian method is very well established in particle physics, where the low-energy effective theory for quantum chromodynamics—chiral perturbation theory—has been constructed a long time ago.[39,40] There, we are dealing with a spontaneously broken chiral symmetry and the corresponding Goldstone bosons are the pseudoscalar mesons. Spontaneous symmetry breaking is also a common phenomenon in condensed matter physics and the effective Lagrangian method has in fact been transferred to this domain[41]: Magnons and phonons, e.g., are the Goldstone bosons resulting from a spontaneously broken spin rotation symmetry $O(3) \to O(2)$ and a spontaneously broken translation symmetry, respectively. In particular, the leading-order effective Lagrangian for the O(3) ferromagnet was constructed in Ref. 41, and the extension to higher orders in the derivative expansion was performed in Refs. 38 and 42.

The paper is organized as follows. Since the systematic effective Lagrangian method is still not very well known within the condensed matter community, in Sec. II we give a brief outline of the method, having in mind the ferromagnet as specific system. In Sec. III A, we briefly review the evaluation of the partition function of an ideal ferromagnet up to order T^5. We then go beyond Dyson's analysis and extend the evaluation to order $T^{11/2}$ in Sec. III B. While the renormalization up to order T^5 is straightforward, the handling of ultraviolet divergences at order $T^{11/2}$ is more involved and is considered in detail in Sec. IV. The low-temperature expansion of the partition function and various thermodynamic quantities is given in Sec. V. Our main result—the low-temperature series for the spontaneous magnetization of an ideal ferromagnet beyond Dyson's analysis—is presented in Sec. VI. Here, we also compare our results with the condensed matter literature. Finally, our conclusions are presented in Sec. VII. Additional information on the effective Lagrangian method for the nonexpert reader may be found in Appendix A. Details on the numerical evaluation of a specific three-loop graph are discussed in Appendix B.

We would like to provide the interested reader with a list of publications that deal with applications of the effective Lagrangian method to condensed matter systems. Applications to systems exhibiting collective magnetic behavior include spin-wave scattering processes,[43] spin-wave mediated nonreciprocal effects in antiferromagnets,[44] antiferromagnets at finite volume[45–48] and finite temperature,[49,50] spin waves in canted phases,[51] and antiferromagnets in two dimensions doped with charge carriers.[52–57] Further applications include phonons,[58] SO(5) invariance and high-T_c-superconductivity,[59] as well as supersolids.[60] Pedagogic introductions to the effective Lagrangian method may be found in Refs. 61– 67.

In particular, we would like to point out that in a recent article on an analytically solvable microscopic model for a hole-doped ferromagnet in $1 + 1$ dimensions,[68] the correctness of the effective field theory approach was demonstrated by comparing the effective theory predictions with the microscopic calculation. Likewise, in a series of high-accuracy investigations of the antiferromagnetic spin-$\frac{1}{2}$ quantum Heisenberg model on a square lattice using the loop-cluster algorithm,[69–72] the Monte Carlo data were confronted with the analytic predictions of magnon chiral perturbation theory and the low-energy constants were extracted with permille accuracy. All these tests unambiguously demonstrate that the effective Lagrangian approach provides a rigorous and systematic derivative expansion for both ferromagnetic and antiferromagnetic systems.

II. SYSTEMATIC LOW-ENERGY EFFECTIVE FIELD THEORY FOR FERROMAGNETIC MAGNONS

The effective Lagrangian method is based on a symmetry analysis of the underlying system. In the present section and in Sec. III A, an overview of the method is given. Still, the nonexpert reader may find it helpful to consult Appendix A,

where additional information on the effective Lagrangian method is provided.

In the present case we study ferromagnets, which are described by the Heisenberg model. Nevertheless, the effective field-theory predictions are model-independent and universal, as they are valid for any system displaying the same symmetries as the Heisenberg ferromagnet. Microscopic details of the system are taken into account through a few low-energy coupling constants in the effective Lagrangian. Symmetry does not fix the actual numerical values of these couplings—in general, these have to be determined experimentally or in a numerical simulation of the underlying model. Symmetry, however, does unambiguously determine the derivative structure of the terms in the effective Lagrangian.

The most important symmetry in the present case is the spontaneously broken spin rotation symmetry: Whereas the Heisenberg model,

$$\mathcal{H}_0 = -J \sum_{n.n.} \vec{S}_m \cdot \vec{S}_n, \qquad J = \text{const.}, \tag{2.1}$$

is invariant under global O(3) spin rotations, the ground state of the ferromagnet ($J > 0$) is invariant under the subgroup O(2) only. According to the nonrelativistic Goldstone theorem,[73–77] we then have one type of spin-wave excitation—or one magnon particle—in the low-energy spectrum of the ferromagnet which obeys a quadratic dispersion relation.

The interaction between an external constant magnetic field $\vec{H} = (0,0,H), H > 0$ and the spin degrees of freedom is taken into account through the Zeeman term. In the corresponding extension of the Heisenberg model,

$$\mathcal{H} = \mathcal{H}_0 - \mu \sum_n \vec{S}_n \cdot \vec{H}, \tag{2.2}$$

the magnetic field couples to the vector of the total spin. The above Hamiltonian, defined on a cubic lattice with purely isotropic exchange coupling between nearest neighbors, represents what Dyson called *ideal* ferromagnet.

Apart from internal symmetries, we also have to consider the various space-time symmetries. Compared to particle physics where we have Lorentz invariance, the situation is more complicated in condensed matter physics, because the center of mass system represents a preferred frame of reference. Moreover, the crystal lattice singles out preferred directions, such that the effective Lagrangian need not be rotationally invariant. In the case of cubic geometry, however, it has been shown that the anisotropies of the lattice start manifesting themselves at higher orders of the derivative expansion[47]—the leading-order effective Lagrangian is thus invariant under space rotations. Moreover, as the effective analysis refers to large wavelengths, it does not resolve the microscopic structure of the crystal: the system appears homogeneous and the effective Lagrangian is also invariant under translations.

The idea underlying the construction of effective Lagrangians is straightforward[78]: One writes down the most general expression consistent with the space-time symmetries and the internal, spontaneously broken symmetry G of the underlying system in terms of Goldstone boson fields $U^a(x), a = 1, \ldots$, dim(G)-dim(H), where the group H refers to the symmetry group of the ground state. The effective Lagrangian then consists of a string of terms involving an increasing number of derivatives or, equivalently, amounts to an expansion in powers of the momentum. Furthermore, the effective Lagrangian method allows us to systematically take into account interactions that explicitly break the symmetry G of the underlying model, provided that they can be treated as perturbations. In the present case, we will include a weak external magnetic field $\vec{H}$.

For the O(3) ferromagnet, the leading-order effective Lagrangian is of order p^2 and takes the form[41]

$$\mathcal{L}^2_{\text{eff}} = \Sigma \frac{\epsilon_{ab} \partial_0 U^a U^b}{1 + U^3} + \Sigma \mu H U^3 - \frac{1}{2} F^2 \partial_r U^i \partial_r U^i. \tag{2.3}$$

The two real components of the magnon field, $U^a (a = 1,2)$, are the first two components of the three-dimensional unit vector $U^i = (U^a, U^3)$, which transforms with the vector representation of the rotation group. While the structure of the above terms is unambiguously determined by the symmetries of the underlying theory, at this order, we have two *a priori* unknown low-energy constants: the spontaneous magnetization Σ and the constant F. The above Lagrangian leads to quadratic dispersion relation

$$\omega(\vec{k}) = \gamma \vec{k}^2 + \mathcal{O}(|\vec{k}|^4), \quad \gamma \equiv \frac{F^2}{\Sigma}, \tag{2.4}$$

obeyed by ferromagnetic magnons. It is important to note that one temporal derivative (∂_0) is on the same footing as two spatial derivatives ($\partial_r \partial_r$)—in the derivative expansion, two powers of momentum thus count as only one power of energy or temperature: $k^2 \propto \omega, T$.

Dyson evaluated the low-temperature expansion of the spontaneous magnetization up to terms of order T^4 or, equivalently, the partition function up to order T^5. This then means that, in the effective Lagrangian framework, we have to consider the expansion of the partition function up to order p^{10}. This calculation was performed in Ref. 38. In the present work, we go one step further and consider the expansion beyond Dyson's analysis, taking into account diagrams of order p^{11}. As it turns out, the corresponding contributions lead to a spin-wave interaction term of order $T^{9/2}$ in the spontaneous magnetization.

The effective Lagrangian method provides us with a simultaneous expansion of physical quantities in powers of the momenta and of the external fields. The essential point is that, to a given order in the low-energy expansion, only a finite number of effective coupling constants and only a finite number of graphs contribute. The leading terms stem from tree graphs, whereas loop graphs only manifest themselves at higher orders in the derivative expansion.[39] So the question arises as to what order in the effective expansion we have to go—i.e., how many derivatives in the effective Lagrangian we have to include and how many loops we have to consider—if we want to evaluate the partition function of a ferromagnet up to order p^{11}.

While loops are suppressed by *two* momentum powers in a Lorentz-invariant framework, it was shown in Ref. 38 that loop corrections involving ferromagnetic magnons are suppressed by *three* momentum powers. Note that we are considering the case of four space-time dimensions. If one lowers the spatial dimension, loops are less suppressed: Loops for ferromagnetic

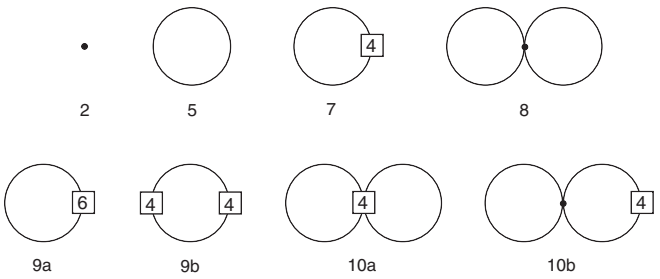

FIG. 1. Feynman graphs related to the low-temperature expansion of the partition function for a ferromagnet up to order p^{10} in dimension $d = 3 + 1$. The numbers attached to the vertices refer to the piece of the effective Lagrangian they come from. Vertices associated with the leading term $\mathcal{L}^2_{\rm eff}$ are denoted by a dot. Note that ferromagnetic loops are suppressed by three-momentum powers in $d = 3 + 1$.

magnons in $d = 2 + 1$, e.g., are suppressed by two momentum powers only. Up to order p^{10}, as depicted in Fig. 1, we thus have to consider graphs which involve two loops at most and have to take into account pieces of the effective Lagrangian involving up to six derivatives. At order p^{11}, as depicted in Fig. 2, three-loop graphs start to show up. At the same time we also have two one-loop graphs that involve vertices from higher-order pieces of the effective Lagrangian: Diagram 11d contains a vertex from $\mathcal{L}^8_{\rm eff}$, while diagram 11e contains insertions from $\mathcal{L}^4_{\rm eff}$ and $\mathcal{L}^6_{\rm eff}$. These five graphs represent the additional diagrams we have to evaluate when we go one step beyond Dyson's analysis.

We now address the question regarding the explicit structure of the pieces $\mathcal{L}^4_{\rm eff}$, $\mathcal{L}^6_{\rm eff}$, and $\mathcal{L}^8_{\rm eff}$. First of all, note that there are no contributions to the effective Lagrangian leading to odd momentum powers: The pieces $\mathcal{L}^3_{\rm eff}, \mathcal{L}^5_{\rm eff}, \ldots$ necessarily involve terms with an odd number of space derivatives like

$$c_{abc}\epsilon_{rst}\partial_r U^a \partial_s U^b \partial_t U^c, \tag{2.5}$$

which are excluded by parity—parity is a discrete symmetry of the underlying Heisenberg model that has to be respected by the effective Lagrangian.

The next-to-leading order Lagrangian is thus of order p^4. It contains terms with two time derivatives, terms with one time and two space derivatives, and terms with four space derivatives. The time derivatives along with the magnetic field, however, can be eliminated with the equation of motion, such that $\mathcal{L}^4_{\rm eff}$ takes the form[38]

$$\mathcal{L}^4_{\rm eff} = l_1(\partial_r U^i \partial_r U^i)^2 + l_2(\partial_r U^i \partial_s U^i)^2 + l_3 \Delta U^i \Delta U^i, \tag{2.6}$$

where Δ denotes the Laplace operator in three dimensions. The next-to-leading order effective Lagrangian hence involves the three effective coupling constants l_1, l_2, and l_3.

An inspection of the diagrams in Figs. 1 and 2 reveals that insertions from $\mathcal{L}^6_{\rm eff}$ and $\mathcal{L}^8_{\rm eff}$ only appear in one-loop graphs: the only terms we need are thus quadratic in the magnon field. Eliminating again time derivatives and terms involving the magnetic field, the pieces relevant for our calculation are

$$\mathcal{L}^6_{\rm eff} = c_1 U^i \Delta^3 U^i, \quad \mathcal{L}^8_{\rm eff} = d_1 U^i \Delta^4 U^i. \tag{2.7}$$

We conclude this section with a remark concerning effects induced by the anisotropy of the lattice. Regarding the cubic lattice, we have mentioned that the anisotropies start manifesting themselves at the four-derivative level: the pieces $\mathcal{L}^4_{\rm eff}$, $\mathcal{L}^6_{\rm eff}$, and $\mathcal{L}^8_{\rm eff}$ indeed contain additional terms—not displayed in Eqs. (2.6) and (2.7)—which are not invariant under space rotations but still invariant under the discrete rotation and reflexion symmetries of the cubic lattice, such as

$$\sum_{s=1,2,3} \partial_s \partial_s U^i \partial_s \partial_s U^i. \tag{2.8}$$

In the present analysis, however, we neglect these extra terms and assume space rotation invariance up to order p^8. The conclusions of the present paper regarding the manifestation of the spin-wave interaction in the partition function are not affected by this idealization: According to Fig. 2, the interaction contribution beyond Dyson is determined by the three-loop graphs of order p^{11}: These graphs only involve the leading-order Lagrangian $\mathcal{L}^2_{\rm eff}$, which is perfectly invariant under space rotations.

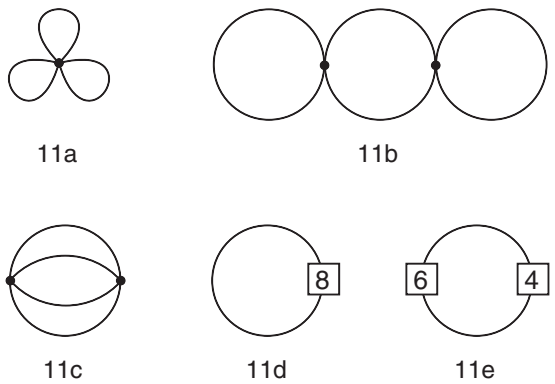

FIG. 2. Feynman graphs related to the low-temperature expansion of the partition function for a ferromagnet at order p^{11} in dimension $d = 3 + 1$. The numbers attached to the vertices refer to the piece of the effective Lagrangian they come from. Vertices associated with the leading term $\mathcal{L}^2_{\rm eff}$ are denoted by a dot.

III. EVALUATION OF THE PARTITION FUNCTION

The low-temperature expansion of the partition function for the O(3) ferromagnet was evaluated in Ref. 38 up to order p^{10}. In Sec. III A, we briefly review some essential features of that calculation. In Sec. III B, we then extend the evaluation of the partition function to order p^{11}. For a review of the effective Lagrangian method at nonzero temperature, the interested reader may consult Ref. 79. For a general review of field theory at finite temperature, see Refs. 80–82.

A. Evaluation up to order p^{10}

In finite-temperature field theory, the partition function is represented as a Euclidean functional integral

$$\mathrm{Tr}[\exp(-\mathcal{H}/T)] = \int [dU] \exp\left(- \int_{\mathcal{T}} d^4x \mathcal{L}_{\rm eff} \right). \tag{3.1}$$

The integration is performed over all field configurations that are periodic in the Euclidean time direction, $U(\vec{x}, x_4 + \beta) =$

$U(\vec{x},x_4)$ with $\beta \equiv 1/T$. The periodicity condition imposed on the magnon fields also reflects itself in the thermal propagator

$$G(x) = \sum_{n=-\infty}^{\infty} \Delta(\vec{x}, x_4 + n\beta), \tag{3.2}$$

where $\Delta(x)$ is the Euclidean propagator at zero temperature,

$$\begin{aligned}\Delta(x) &= \int \frac{dk_4 d^3k}{(2\pi)^4} \frac{e^{i\vec{k}\vec{x} - ik_4x_4}}{\gamma\vec{k}^2 - ik_4 + \mu H} \\ &= \Theta(x_4) \int \frac{d^3k}{(2\pi)^3} e^{i\vec{k}\vec{x} - \gamma\vec{k}^2x_4 - \mu H x_4}.\end{aligned} \tag{3.3}$$

An explicit representation for the thermal propagator, dimensionally regularized in the spatial dimension d_s, is

$$G(x) = \frac{1}{(2\pi)^{d_s}} \left(\frac{\pi}{\gamma}\right)^{\frac{d_s}{2}} \sum_{n=-\infty}^{\infty} \frac{1}{x_n^{\frac{d_s}{2}}} \exp^{-\frac{\vec{x}^2}{4\gamma x_n} - \mu H x_n} \Theta(x_n), \tag{3.4}$$

with

$$x_n \equiv x_4 + n\beta. \tag{3.5}$$

We restrict ourselves to the infinite volume limit and evaluate the free energy density z, defined by

$$z = -T \lim_{L\to\infty} L^{-3} \ln[\mathrm{Tr} \exp(-\mathcal{H}/T)]. \tag{3.6}$$

In the evaluation of the various Feynman diagrams, we will repeatedly be dealing with thermal propagators (and space derivatives thereof), which have to be evaluated at the origin. It is convenient to introduce the following notation,

$$\begin{aligned} G_1 \equiv [G(x)]_{x=0}, \quad G_\Delta \equiv [\Delta G(x)]_{x=0}, \\ G_{\Delta^n} \equiv [\Delta^n G(x)]_{x=0}, \end{aligned} \tag{3.7}$$

where Δ represents the Laplace operator in the spatial dimensions—no confusion should occur with $\Delta(x)$, which denotes the zero-temperature propagator.

The quantities G_1, G_Δ, as well as thermal propagators involving higher-order space derivatives, are split into a finite piece, which is temperature dependent, and a divergent piece, which is temperature independent,

$$G_1 = G_1^T + G_1^0, \quad G_\Delta = G_\Delta^T + G_\Delta^0. \tag{3.8}$$

The explicit expressions can be found in Ref. 38 and will not be given here. Rather, we would like to point out two important observations, which lead to a substantial simplification of the renormalization procedure. First, the temperature-independent pieces $G_1^0, G_\Delta^0, \ldots$ are all related to momentum integrals of the form

$$\int d^{d_s}k (\vec{k}^2)^m \exp\big[-\gamma x_4 \vec{k}^2 - x_4 \mu H\big] \quad m = 0,1,2,\ldots, \tag{3.9}$$

which are proportional to

$$\frac{\exp[-x_4\mu H]}{(\gamma x_4)^{m+\frac{d_s}{2}}} \Gamma\left(m + \frac{d_s}{2}\right). \tag{3.10}$$

In dimensional regularization, these expressions vanish altogether: G_1^0, G_Δ^0, and zero-temperature propagators involving higher-order space derivatives do not contribute in the limit $d_s \to 3$.

The second observation concerns the fact that, up to order p^{10}, the individual contributions to the free energy density from the various diagrams factorize into products of thermal propagators (involving space derivatives or derivatives with respect to the magnetic field), which all have to be evaluated at the origin. As an example, consider the two-loop graph 10a, which yields the contribution

$$z_{10a} = -\frac{2}{3\Sigma^2}(8l_1 + 6l_2 + 5l_3) G_\Delta G_\Delta - \frac{2l_3}{\Sigma^2} G_1 G_{\Delta^2}. \tag{3.11}$$

According to the first observation regarding dimensional regularization, it is then clear that in the two products of thermal propagators above only the fully temperature-dependent pieces—$G_\Delta^T G_\Delta^T$ and $G_1^T G_{\Delta^2}^T$—are nonzero, whereas any other terms involving temperature-independent pieces of propagators vanish identically. We thus conclude that, using dimensional regularization, the renormalization of the partition function up to order p^{10} is quite trivial. As we will see in the next subsection, the renormalization at the three-loop level, on the other hand, is more complicated but still perfectly feasible within the effective field theory framework.

Without going into more details (the interested reader may consult Ref. 38), we present the final result for the free energy density of the O(3) ferromagnet up to order p^{10}:

$$\begin{aligned} z = &-\Sigma\mu H - \frac{1}{8\pi^{\frac{3}{2}}\gamma^{\frac{3}{2}}} T^{\frac{5}{2}} \sum_{n=1}^{\infty} \frac{e^{-\mu H n\beta}}{n^{\frac{5}{2}}} \\ &- \frac{15 l_3}{16\pi^{\frac{3}{2}}\Sigma\gamma^{\frac{7}{2}}} T^{\frac{7}{2}} \sum_{n=1}^{\infty} \frac{e^{-\mu H n\beta}}{n^{\frac{7}{2}}} \\ &- \frac{105}{32\pi^{\frac{3}{2}}\Sigma\gamma^{\frac{9}{2}}} \left(\frac{9l_3^2}{2\gamma\Sigma} - c_1\right) T^{\frac{9}{2}} \sum_{n=1}^{\infty} \frac{e^{-\mu H n\beta}}{n^{\frac{9}{2}}} \\ &- \frac{3(8l_1 + 6l_2 + 5l_3)}{128\pi^3\Sigma^2\gamma^5} T^5 \left\{ \sum_{n=1}^{\infty} \frac{e^{-\mu H n\beta}}{n^{\frac{5}{2}}} \right\}^2 \\ &+ \mathcal{O}(T^{\frac{11}{2}}). \end{aligned} \tag{3.12}$$

The first term in this series does not depend on temperature and originates from the tree graph 2 (see Fig. 1). The terms which involve half-integer powers of the temperature—$T^{5/2}, T^{7/2}$, and $T^{9/2}$, respectively—arise from the one-loop graphs displayed in Fig. 1. They all contribute to the free energy density of noninteracting magnons. Remarkably, up to order p^{10}, there is only one term in the above series—the contribution of order T^5 coming from the two-loop graphs 10a and 10b—which is due to the magnon-magnon interaction.

In particular, there is no term of order T^4 in the above series for the free energy density: The two-loop graph 8, which would be the only candidate to yield such a contribution, is proportional to single space derivatives of the thermal propagator evaluated at the origin:

$$z_8 \propto [\partial_r G(x)]_{x=0} [\partial_r G(x)]_{x=0} = 0. \tag{3.13}$$

This contribution vanishes due to space rotation invariance of the leading-order effective Lagrangian.

B. Evaluation at order p^{11}

According to Fig. 2, we have a total of five diagrams at order p^{11}. We first consider the two one-loop graphs, which involve vertices from $\mathcal{L}^4_{\rm eff}$, $\mathcal{L}^6_{\rm eff}$, and $\mathcal{L}^8_{\rm eff}$. For graph 11d we obtain

$$z_{11d} = -\frac{2d_1}{\Sigma} G_{\Delta^4}, \tag{3.14}$$

yielding the temperature-dependent contribution

$$z^T_{11d} = -\frac{945 d_1}{64\pi^{\frac{3}{2}}\Sigma\gamma^{\frac{11}{2}}} T^{\frac{11}{2}} \sum_{n=1}^{\infty} \frac{e^{-\mu H n\beta}}{n^{\frac{11}{2}}}. \tag{3.15}$$

Graph 11e is proportional to an integral over the torus $\mathcal{T} = \mathcal{R}^{d_s} \times S^1$, with circle S^1 defined by $-\beta/2 \leqslant x_4 \leqslant \beta/2$, and involves a product of two thermal propagators,

$$z_{11e} = -\frac{4 l_3 c_1}{\Sigma^2} \int_{\mathcal{T}} d^{d_s+1}x \, \Delta^2 G(x) \Delta^3 G(-x). \tag{3.16}$$

This integral, however, can be reduced to an expression involving one propagator only, using the relation[38]

$$\left[\Delta^{(m+n)} \frac{\partial G(x)}{\partial(\mu H)}\right]_{x=0} = -\int_{\mathcal{T}} d^{d_s+1}y \, \Delta^m G(-y) \Delta^n G(y). \tag{3.17}$$

We then end up with

$$z_{11e} = \frac{4 l_3 c_1}{\Sigma^2} \left[\Delta^5 \frac{\partial G(x)}{\partial(\mu H)}\right]_{x=0}. \tag{3.18}$$

Accordingly, the temperature-dependent part of graph 11e reads

$$z^T_{11e} = \frac{10395 l_3 c_1}{64\pi^{\frac{3}{2}}\Sigma^2\gamma^{\frac{13}{2}}} T^{\frac{11}{2}} \sum_{n=1}^{\infty} \frac{e^{-\mu H n\beta}}{n^{\frac{11}{2}}}. \tag{3.19}$$

We now turn to the three-loop graphs—note that they exclusively contain vertices from the leading-order Lagrangian $\mathcal{L}^2_{\rm eff}$. Graph 11a factorizes into a product of three thermal propagators (and space derivatives thereof), to be evaluated at the origin,

$$z_{11a} = -\frac{F^2}{\Sigma^3} G_\Delta (G_1)^2. \tag{3.20}$$

The subsequent three-loop graph 11b, remarkably, does not contribute to the partition function,

$$z_{11b} = 0. \tag{3.21}$$

As it was the case for the two-loop graph 8, the three-loop graph 11b is identically zero.

Finally, for the cateye graph 11c, we get

$$z_{11c} = -\frac{F^4}{2\Sigma^4} J + \frac{F^2}{\Sigma^3} G_\Delta (G_1)^2. \tag{3.22}$$

The expression J stands for the following integral over the torus involving a product of four thermal propagators:

$$J = \int_{\mathcal{T}} d^{d_s+1}x \, \partial_r G \partial_r G \partial_s \tilde{G} \partial_s \tilde{G}, \tag{3.23}$$

where we have used the notation

$$G = G(x), \quad \tilde{G} = G(-x). \tag{3.24}$$

Note that the second term in (3.22) cancels the contribution from graph 11a, such that the overall contribution from the three-loop graphs is the one proportional to the integral J. Remarkably, unlike all other pieces in the free energy density up to order p^{11}, this quantity is not just a product of thermal propagators (or derivatives thereof) to be evaluated at the origin. The remaining task will be the renormalization and the numerical evaluation of this integral, which contains a total of four infinite sums. In the next section and in Appendix B, we address this problem in detail.

Leaving aside these technical issues for a moment, we note that the cateye graph of order p^{11} will lead to a term of order $T^{11/2}$ in the free energy density,

$$J \propto T^{\frac{11}{2}}. \tag{3.25}$$

Hence, the spin-wave interaction in the low-temperature series of the free energy density—beyond Dyson's T^5-term—already manifests itself at order $T^{11/2}$. It is remarkable that this contribution is exclusively determined by the symmetries of the leading-order effective Lagrangian $\mathcal{L}^2_{\rm eff}$, which involves the two couplings Σ and F—the spin-wave interaction at this order is not affected by the anisotropies of the cubic lattice.

IV. RENORMALIZATION OF THE CATEYE GRAPH

Using dimensional regularization, it was straightforward to extract the finite pieces in the partition function up to two-loop order p^{10}. The renormalization of the three-loop graph 11c, on the other hand, is more involved. We will follow the procedure outlined in Ref. 83, where the same graph was considered in the context of a Lorentz-invariant effective field theory.

To analyze the integral

$$J = \int_{\mathcal{T}} d^{d_s+1}x \, \partial_r G \partial_r G \partial_s \tilde{G} \partial_s \tilde{G}$$

in the limit $d_s \to 3$, we split the thermal propagator into two pieces

$$G(x) = G^T(x) + \Delta(x). \tag{4.1}$$

The ultraviolet singularities are contained in the zero-temperature propagator $\Delta(x)$, whereas the temperature-dependent part $G^T(x)$ is finite as $d_s \to 3$. Note that, if we restrict ourselves to the origin, we reproduce the first relation of Eq. (3.8).

Inserting the above decomposition into the integral J, we end up with nine terms that can be grouped into the following six classes—for simplicity we do not display the derivatives:

$$\begin{aligned}
&A: G^T(x)G^T(x)G^T(-x)G^T(-x),\\
&B: \Delta(x)G^T(x)G^T(-x)G^T(-x),\\
&\quad\ G^T(x)G^T(x)\Delta(-x)G^T(-x),\\
&C: \Delta^2(x)G^T(-x)G^T(-x), G^T(x)G^T(x)\Delta^2(-x),\\
&D: \Delta(x)G^T(x)\Delta(-x)G^T(-x),\\
&E: \Delta^2(x)\Delta(-x)G^T(-x), \Delta(x)G^T(x)\Delta^2(-x),\\
&F: \Delta^2(x)\Delta^2(-x).
\end{aligned} \tag{4.2}$$

Terms of the classes D, E, and F vanish identically since the product $\Delta(x)\Delta(-x)$ of zero-temperature propagators involves the combination $\Theta(x_4)\Theta(-x_4)$. The maximum number of Θ

functions a given term can contain—in order not to be zero—is two. Moreover, the arguments of the two Θ functions have to coincide as it is the case with the terms of class C. We thus have to consider the cases A, B, and C.

The integral over the torus involving contributions of classes A and B,

$$\int_{\mathcal{T}} d^{d_s+1}x \left(\partial_r G^T \partial_r G^T \partial_s \tilde{G}^T \partial_s \tilde{G}^T + 4\partial_r \Delta \partial_r G^T \partial_s \tilde{G}^T \partial_s \tilde{G}^T\right), \tag{4.3}$$

converges at $d_s = 3$.

Terms of class C, however, do lead to an ultraviolet-divergent integral. Consider, e.g., the term

$$\partial_r \Delta(x) \partial_r \Delta(x) \partial_s G^T(-x) \partial_s G^T(-x), \tag{4.4}$$

where we now have displayed the derivatives. For the zero-temperature piece $\partial_r \Delta(x)$ we have

$$\partial_r \Delta(x) \propto \frac{x^r}{x_4^{\frac{5}{2}}} \exp\left[-\frac{\vec{x}^2}{4\gamma x_4}\right]. \tag{4.5}$$

The Taylor series of the function $\partial_s G^T(-x)$, evaluated at the origin, starts with a term linear in $\vec{x}$,

$$\partial_s G^T(-x) = \partial_{\alpha s} G^T(-x)|_{x=0} x^\alpha + \mathcal{O}(\vec{x}^3). \tag{4.6}$$

Inserting this term into Eq. (4.4), we end up with the following contribution in J,

$$J \propto \int d^3x dx_4 \left(\frac{\vec{x}}{x_4^{\frac{5}{2}}}\right)^2 e^{-\vec{x}^2/2\gamma x_4} \vec{x}^2 \quad \propto \int dx_4 \frac{1}{x_4^{\frac{3}{2}}}, \tag{4.7}$$

which is singular in the ultraviolet. On the other hand, one readily checks that this term in fact is the only one that has to be subtracted: The cubic Taylor term in the expansion of $\partial_s \tilde{G}^T$, Eq. (4.6), already leads to a convergent contribution to the integral J. We now discuss the renormalization procedure in detail, along the lines of Ref. 83, which we adapt to nonrelativistic kinematics.

We first cut out a sphere $\mathcal{S}$ of radius $|\mathcal{S}| \leqslant \beta/2$ around the origin and decompose the integral involving the contributions of class C according to

$$\begin{aligned}\int_{\mathcal{T}} d^{d_s+1}x \partial_r \Delta \partial_r \Delta \partial_s \tilde{G}^T \partial_s \tilde{G}^T &= \int_{\mathcal{S}} d^{d_s+1}x \partial_r \Delta \partial_r \Delta \partial_s \tilde{G}^T \partial_s \tilde{G}^T \\ &+ \int_{\mathcal{T}\setminus\mathcal{S}} d^{d_s+1}x \partial_r \Delta \partial_r \Delta \partial_s \tilde{G}^T \partial_s \tilde{G}^T.\end{aligned} \tag{4.8}$$

The integral over the complement $\mathcal{T} \setminus \mathcal{S}$ of the sphere is not singular in the limit $d_s \to 3$. In the integral over the sphere, which is divergent, we subtract the singular term discussed above, arriving at

$$\begin{aligned}\int_{\mathcal{S}} d^{d_s+1}x \partial_r \Delta(x) \partial_r \Delta(x) \partial_s G^T(-x) \partial_s G^T(-x) &= \int_{\mathcal{S}} d^{d_s+1}x \partial_r \Delta(x) \partial_r \Delta(x) Q_{ss}(x) \\ &+ \int_{\mathcal{S}} d^{d_s+1}x \partial_r \Delta(x) \partial_r \Delta(x) \\ &\times \partial_{\alpha s} G^T(-x)|_{x=0} \partial_{\beta s} G^T(-x)|_{x=0} x^\alpha x^\beta,\end{aligned} \tag{4.9}$$

where the quantity $Q_{ss}(x)$ is defined as

$$\begin{aligned}Q_{ss}(x) &= \partial_s G^T(-x) \partial_s G^T(-x) \\ &- \partial_{\alpha s} G^T(-x)|_{x=0} \partial_{\beta s} G^T(-x)|_{x=0} x^\alpha x^\beta.\end{aligned} \tag{4.10}$$

Whereas in Eq. (4.9) the first integral on the right hand side now is convergent, the second integral does contain the ultraviolet singularity. The last step in the isolation of this singularity consists in decomposing the respective integral as follows:

$$\begin{aligned}&\int_{\mathcal{S}} d^{d_s+1}x \partial_r \Delta(x) \partial_r \Delta(x) \partial_{\alpha s} G^T(-x)|_{x=0} \partial_{\beta s} G^T(-x)|_{x=0} x^\alpha x^\beta \\ &= \int_{\mathcal{R}} d^{d_s+1}x \partial_r \Delta(x) \partial_r \Delta(x) \partial_{\alpha s} G^T(-x)|_{x=0} \\ &\times \partial_{\beta s} G^T(-x)|_{x=0} x^\alpha x^\beta \\ &- \int_{\mathcal{R}\setminus\mathcal{S}} d^{d_s+1}x \partial_r \Delta(x) \partial_r \Delta(x) \partial_{\alpha s} G^T(-x)|_{x=0} \\ &\times \partial_{\beta s} G^T(-x)|_{x=0} x^\alpha x^\beta.\end{aligned} \tag{4.11}$$

The UV singularity is contained in the integral over all Euclidean space, which can be cast into the form

$$\begin{aligned}&\int_{\mathcal{R}} d^{d_s+1}x \partial_r \Delta(x) \partial_r \Delta(x) \partial_{\alpha s} G^T(-x)|_{x=0} \partial_{\beta s} G^T(-x)|_{x=0} \\ &\times x^\alpha x^\beta = \frac{d_s(d_s+2)}{2^{3d_s+5}\pi^{\frac{3d_s}{2}}\gamma^{\frac{3d_s+4}{2}}} T^{d_s+2} (\mu H)^{\frac{d_s-2}{2}} \\ &\times \left\{\sum_{n=1}^{\infty} \frac{e^{-\mu H n \beta}}{n^{\frac{d_s+2}{2}}}\right\}^2 \Gamma\left(1-\frac{d_s}{2}\right).\end{aligned} \tag{4.12}$$

In the limit $d_s \to 3$, the above regularized expression is finite and takes the value

$$-\frac{15}{8192\pi^4\gamma^{\frac{13}{2}}} T^{\frac{11}{2}} \sqrt{\sigma} \left\{\sum_{n=1}^{\infty} \frac{e^{-\sigma n}}{n^{\frac{5}{2}}}\right\}^2, \tag{4.13}$$

where we have defined the dimensionless quantity σ as

$$\sigma = \mu H \beta = \frac{\mu H}{T}. \tag{4.14}$$

Collecting the various contributions, we arrive at the following representation for the renormalized integral $\bar{J}$:

$$\begin{aligned}\bar{J} &= \int_{\mathcal{T}} d^4x \left(\partial_r G^T \partial_r G^T \partial_s \tilde{G}^T \partial_s \tilde{G}^T + 4\partial_r \Delta \partial_r G^T \partial_s \tilde{G}^T \partial_s \tilde{G}^T\right) \\ &+ 2\int_{\mathcal{T}\setminus\mathcal{S}} d^4x \partial_r \Delta \partial_r \Delta \partial_s \tilde{G}^T \partial_s \tilde{G}^T + 2\int_{\mathcal{S}} d^4x \partial_r \Delta \partial_r \Delta Q_{ss} \\ &- 2\int_{\mathcal{R}\setminus\mathcal{S}} d^4x \partial_r \Delta \partial_r \Delta \partial_{\alpha s} G^T(-x)|_{x=0} \partial_{\beta s} G^T(-x)|_{x=0} x^\alpha x^\beta \\ &- \frac{15}{4096\pi^4\gamma^{\frac{13}{2}}} T^{\frac{11}{2}} \sqrt{\sigma} \left\{\sum_{n=1}^{\infty} \frac{e^{-\sigma n}}{n^{\frac{5}{2}}}\right\}^2.\end{aligned} \tag{4.15}$$

Note that all terms therein are well-defined at the physical dimension $d_s = 3$.

Since the various integrands only depend on the variables $r = |\vec{x}|$ and $t = x_4$, the integrals become, in fact, two-dimensional,

$$d^4x = 4\pi r^2 dr dt, \tag{4.16}$$

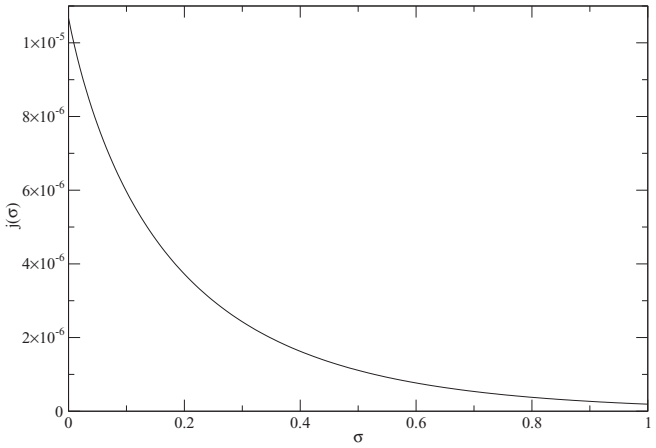

FIG. 3. The function $j(\sigma)$, where σ is the dimensionless parameter $\sigma = \mu H/T$.

and the numerical evaluation of the integral $\bar{J}$ is straightforward. A very welcome consistency check on the numerics is provided by the fact that the result must be independent of the radius of the sphere $\mathcal{S}$. While more details concerning the numerical evaluation can be found in Appendix B, in the next section we discuss the result for the function $\bar{J} = \bar{J}(\sigma)$. In particular, we consider the limit $\sigma \to 0$, which is needed for the evaluation of the spontaneous magnetization.

V. THERMODYNAMICS OF THE IDEAL FERROMAGNET

For dimensional reasons, the renormalized integral $\bar{J}$ can be written as

$$\bar{J}(\sigma) = T^{\frac{11}{2}} \frac{j(\sigma)}{\gamma^{\frac{13}{2}}}, \quad \sigma = \frac{\mu H}{T}, \quad \gamma = \frac{F^2}{\Sigma}, \tag{5.1}$$

where the quantity $j(\sigma)$ is a dimensionless function. A graph is provided in Fig. 3.

In the limit $\sigma \to 0$, the function can be parametrized by

$$j(\sigma) = j_1 + j_2\sigma + \mathcal{O}(\sigma^{3/2}). \tag{5.2}$$

The coefficients j_1 and j_2 are pure numbers given by

$$j_1 = 1.07 \times 10^{-5}, \quad j_2 = -8 \times 10^{-5}. \tag{5.3}$$

It should be noted that, in the limit $\sigma \to 0$, the last two contributions in Eq. (4.15) contain terms involving the square root $\sqrt{\sigma}$. Since they have opposite signs, however, they cancel each other.

With the above representation for the quantity $j(\sigma)$, the final result for the low-temperature expansion of free energy density for the ideal ferromagnet up to order p^{11} takes the form

$$\begin{aligned} z = &-\Sigma\mu H - \frac{1}{8\pi^{\frac{3}{2}}\gamma^{\frac{3}{2}}} T^{\frac{5}{2}} \sum_{n=1}^{\infty} \frac{e^{-\mu Hn\beta}}{n^{\frac{5}{2}}} \\ &- \frac{15l_3}{16\pi^{\frac{3}{2}}\Sigma\gamma^{\frac{7}{2}}} T^{\frac{7}{2}} \sum_{n=1}^{\infty} \frac{e^{-\mu Hn\beta}}{n^{\frac{7}{2}}} \\ &- \frac{105}{32\pi^{\frac{3}{2}}\Sigma\gamma^{\frac{9}{2}}} \left(\frac{9l_3^2}{2\Sigma\gamma} - c_1 \right) T^{\frac{9}{2}} \sum_{n=1}^{\infty} \frac{e^{-\mu Hn\beta}}{n^{\frac{9}{2}}} \\ &- \frac{3(8l_1 + 6l_2 + 5l_3)}{128\pi^3\Sigma^2\gamma^5} T^5 \left\{ \sum_{n=1}^{\infty} \frac{e^{-\mu Hn\beta}}{n^{\frac{5}{2}}} \right\}^2 \\ &- \frac{945d_1}{64\pi^{\frac{3}{2}}\Sigma\gamma^{\frac{11}{2}}} T^{\frac{11}{2}} \sum_{n=1}^{\infty} \frac{e^{-\mu Hn\beta}}{n^{\frac{11}{2}}} \\ &+ \frac{10395l_3c_1}{64\pi^{\frac{3}{2}}\Sigma^2\gamma^{\frac{13}{2}}} T^{\frac{11}{2}} \sum_{n=1}^{\infty} \frac{e^{-\mu Hn\beta}}{n^{\frac{11}{2}}} \\ &- \frac{1}{2\Sigma^2\gamma^{\frac{9}{2}}} j(\mu H\beta) T^{\frac{11}{2}} + \mathcal{O}(T^6). \end{aligned} \tag{5.4}$$

Because the system is homogeneous, the pressure can be obtained from the temperature-dependent part of the free energy density,

$$P = z_0 - z. \tag{5.5}$$

Accordingly, up to order p^{11}, the low-temperature series for the pressure reads

$$P = h_0 T^{\frac{5}{2}} + h_1 T^{\frac{7}{2}} + h_2 T^{\frac{9}{2}} + h_3 T^5 + h_4 T^{\frac{11}{2}} + \mathcal{O}(T^6), \tag{5.6}$$

where the coefficients h_i are given by

$$\begin{aligned} h_0 &= \frac{1}{8\pi^{\frac{3}{2}}\gamma^{\frac{3}{2}}} \sum_{n=1}^{\infty} \frac{e^{-\mu Hn\beta}}{n^{\frac{5}{2}}}, \\ h_1 &= \frac{15l_3}{16\pi^{\frac{3}{2}}\Sigma\gamma^{\frac{7}{2}}} \sum_{n=1}^{\infty} \frac{e^{-\mu Hn\beta}}{n^{\frac{7}{2}}}, \\ h_2 &= \frac{105}{32\pi^{\frac{3}{2}}\Sigma\gamma^{\frac{9}{2}}} \left(\frac{9l_3^2}{2\Sigma\gamma} - c_1 \right) \sum_{n=1}^{\infty} \frac{e^{-\mu Hn\beta}}{n^{\frac{9}{2}}}, \\ h_3 &= \frac{3(8l_1 + 6l_2 + 5l_3)}{128\pi^3\Sigma^2\gamma^5} \left\{ \sum_{n=1}^{\infty} \frac{e^{-\mu Hn\beta}}{n^{\frac{5}{2}}} \right\}^2, \\ h_4 &= \frac{945}{64\pi^{\frac{3}{2}}\Sigma\gamma^{\frac{11}{2}}} \left(d_1 - \frac{11l_3c_1}{\Sigma\gamma} \right) \sum_{n=1}^{\infty} \frac{e^{-\mu Hn\beta}}{n^{\frac{11}{2}}} + \frac{1}{2\Sigma^2\gamma^{\frac{9}{2}}} j. \end{aligned} \tag{5.7}$$

In the limit $\sigma = \mu H/T \to 0$, these coefficients become temperature independent and the sums reduce to Riemann zeta functions,

$$\begin{aligned} \tilde{h}_0 &= \frac{1}{8\pi^{\frac{3}{2}}\gamma^{\frac{3}{2}}} \zeta\left(\frac{5}{2}\right), \\ \tilde{h}_1 &= \frac{15l_3}{16\pi^{\frac{3}{2}}\Sigma\gamma^{\frac{7}{2}}} \zeta\left(\frac{7}{2}\right), \\ \tilde{h}_2 &= \frac{105}{32\pi^{\frac{3}{2}}\Sigma\gamma^{\frac{9}{2}}} \left(\frac{9l_3^2}{2\Sigma\gamma} - c_1 \right) \zeta\left(\frac{9}{2}\right), \\ \tilde{h}_3 &= \frac{3(8l_1 + 6l_2 + 5l_3)}{128\pi^3\Sigma^2\gamma^5} \zeta^2\left(\frac{5}{2}\right), \\ \tilde{h}_4 &= \frac{945}{64\pi^{\frac{3}{2}}\Sigma\gamma^{\frac{11}{2}}} \left(d_1 - \frac{11l_3c_1}{\Sigma\gamma} \right) \zeta\left(\frac{11}{2}\right) + \frac{1}{2\Sigma^2\gamma^{\frac{9}{2}}} j_1. \end{aligned} \tag{5.8}$$

The spin-wave interaction manifests itself in the last two terms involving the coefficients $\tilde{h}_3$ and $\tilde{h}_4$. The contribution proportional to five powers of the temperature in the pressure is the famous Dyson term. In the effective theory, it originates from the two-loop graphs 10a and 10b of Fig. 1. Our main new

result concerns the manifestation of the spin-wave interaction beyond Dyson: the leading correction in the pressure is of order $T^{11/2}$. It is contained in the last term of the coefficient $\tilde{h}_4$ and stems from the three-loop graph 11c.

Note that all other contributions in the pressure up to order p^{11} originate from one-loop graphs—those graphs describe noninteracting magnons and merely modify the dispersion relation. In the above series for the pressure, they involve half-integer powers of the temperature: $T^{5/2}, T^{7/2}, T^{9/2}$, and $T^{11/2}$.

We have to point out that the sign of the Dyson term of order T^5 is not determined by the symmetries—the low-energy constants l_1,l_2, and l_3 appearing in the coefficient $\tilde{h}_3$ may take positive or negative values, depending on the specific underlying model. For the present case of the Heisenberg model, however, Dyson has derived an explicit microscopic expression for $\tilde{h}_3$. As it turns out, for all three types of cubic lattices, this coefficient is positive, leading to a positive contribution to the pressure. We thus conclude that the spin-wave interaction in the ideal ferromagnet is repulsive at low temperatures.

Remarkably, while the sign of the coefficient of order T^5 is not determined within the effective theory framework, the sign of the coefficient of the subsequent interaction contribution of order $T^{11/2}$ is unambiguously fixed: the last term in $\tilde{h}_4$ only involves the coupling constants of the leading-order effective Lagrangian $\mathcal{L}^2_{\text{eff}}$ and the coefficient j_1, which is a pure number—the conditions imposed by symmetry are thus very restrictive here. Since the numerical value of j_1 is positive, the corresponding contribution to the pressure is positive as well, enhancing thus the weak repulsive interaction between spin waves at low temperatures.

Finally, let us consider the low-temperature series for the energy density u, for the entropy density s, and for the heat capacity c_V of the O(3) ferromagnet. They are readily worked out from the thermodynamic relations

$$s = \frac{\partial P}{\partial T},\ u = Ts - P,\ c_V = \frac{\partial u}{\partial T} = T\frac{\partial s}{\partial T}. \tag{5.9}$$

In the limit $\sigma \to 0$, we obtain

$$\begin{aligned} u &= \tfrac{3}{2}\tilde{h}_0 T^{\frac{5}{2}} + \tfrac{5}{2}\tilde{h}_1 T^{\frac{7}{2}} + \tfrac{7}{2}\tilde{h}_2 T^{\frac{9}{2}} + 4\tilde{h}_3 T^5 \\ &\quad + \tfrac{9}{2}\tilde{h}_4 T^{\frac{11}{2}} + \mathcal{O}(T^6), \\ s &= \tfrac{5}{2}\tilde{h}_0 T^{\frac{3}{2}} + \tfrac{7}{2}\tilde{h}_1 T^{\frac{5}{2}} + \tfrac{9}{2}\tilde{h}_2 T^{\frac{7}{2}} + 5\tilde{h}_3 T^4 \\ &\quad + \tfrac{11}{2}\tilde{h}_4 T^{\frac{9}{2}} + \mathcal{O}(T^5), \\ c_V &= \tfrac{15}{4}\tilde{h}_0 T^{\frac{3}{2}} + \tfrac{35}{4}\tilde{h}_1 T^{\frac{5}{2}} + \tfrac{63}{4}\tilde{h}_2 T^{\frac{7}{2}} + 20\tilde{h}_3 T^4 \\ &\quad + \tfrac{99}{4}\tilde{h}_4 T^{\frac{9}{2}} + \mathcal{O}(T^5). \end{aligned} \tag{5.10}$$

Again, the correction to Dyson's result is contained in the respective last terms in the above series involving the coefficient $\tilde{h}_4$.

VI. SPONTANEOUS MAGNETIZATION: EFFECTIVE FRAMEWORK VERSUS CONDENSED MATTER LITERATURE

We now turn to the discussion of the general structure of the low-temperature series for the spontaneous magnetization of the ideal ferromagnet. While this problem has attracted more than a hundred authors over the past few decades, to the best of our knowledge, a rigorous and fully systematic calculation of higher-order corrections to the Dyson term has never been achieved. Before we review the relevant results in the literature, let us analyze the problem within the systematic effective field theory framework.

With the expression for the free energy density (5.4), the low-temperature expansion for the spontaneous magnetization

$$\Sigma(T) = -\lim_{H\to 0}\frac{\partial z}{\partial(\mu H)} \tag{6.1}$$

of the O(3) ferromagnet, up to order $T^{9/2}$, takes the form

$$\begin{aligned} \frac{\Sigma(T)}{\Sigma} &= 1 - \alpha_0 T^{\frac{3}{2}} - \alpha_1 T^{\frac{5}{2}} - \alpha_2 T^{\frac{7}{2}} \\ &\quad - \alpha_3 T^4 - \alpha_4 T^{\frac{9}{2}} + \mathcal{O}(T^5). \end{aligned} \tag{6.2}$$

The coefficients α_i are independent of the temperature and given by

$$\begin{aligned} \alpha_0 &= \frac{1}{8\pi^{\frac{3}{2}}\Sigma\gamma^{\frac{3}{2}}}\zeta\left(\frac{3}{2}\right), \\ \alpha_1 &= \frac{15 l_3}{16\pi^{\frac{3}{2}}\Sigma^2\gamma^{\frac{7}{2}}}\zeta\left(\frac{5}{2}\right), \\ \alpha_2 &= \frac{105}{32\pi^{\frac{3}{2}}\Sigma^2\gamma^{\frac{9}{2}}}\left(\frac{9l_3^2}{2\Sigma\gamma} - c_1\right)\zeta\left(\frac{7}{2}\right), \\ \alpha_3 &= \frac{3(8l_1 + 6l_2 + 5l_3)}{64\pi^3\Sigma^3\gamma^5}\zeta\left(\frac{5}{2}\right)\zeta\left(\frac{3}{2}\right), \\ \alpha_4 &= \frac{945}{64\pi^{\frac{3}{2}}\Sigma^2\gamma^{\frac{11}{2}}}\left(d_1 - \frac{11 l_3 c_1}{\Sigma\gamma}\right)\zeta\left(\frac{9}{2}\right) - \frac{1}{2\Sigma^3\gamma^{\frac{9}{2}}}j_2. \end{aligned} \tag{6.3}$$

Up to order T^4, we reproduce Dyson's series—this calculation was presented in detail in Ref. 38. In the effective Lagrangian framework, the famous interaction term of order T^4 in the spontaneous magnetization originates from the two-loop graphs 10a and 10b, which involve vertices from the next-to-leading order Lagrangian $\mathcal{L}^4_{\text{eff}}$. Note that there is no interaction term of order T^3 in the above series.

Our main new result concerns the leading correction to Dyson's term, which originates from the three-loop graph 11c. The correction in the spontaneous magnetization is of order $T^{9/2}$. Remarkably, the corresponding coefficient—the last term in α_4—does not involve any higher-order low-energy constants. It only involves Σ and F, as well as the coefficient j_2, which is a pure number determined by the symmetries of the underlying Heisenberg model. Since the coefficient j_2 is negative, this contribution has the same sign as the Dyson coefficient α_3. The effect of the three-loop contribution is thus to enhance the weak spin-wave interaction found by Dyson.

Apart from these two interaction terms of order T^4 and $T^{9/2}$, respectively, all other temperature-dependent contributions to the spontaneous magnetization originate from one-loop

graphs, which describe noninteracting magnons. They merely modify the dispersion relation or—as Dyson expressed it[6]—they merely arise "from the discreteness of the lattice, are easy to calculate, and are not of any theoretical interest." In the above series for the spontaneous magnetization, they involve half-integer powers of the temperature: $T^{3/2}, T^{5/2}, T^{7/2}$, and $T^{9/2}$.

It should be pointed out that the contribution of order $T^{9/2}$ contains two parts: The first term in the coefficient α_4 is due to two one-loop graphs associated with noninteracting magnons. The second term is due to a three-loop graph and represents the dominant spin-wave interaction term beyond Dyson. Note that the Dyson coefficient α_3, on the other hand, exclusively involves an interaction part.

Here comes the appropriate place to compare our results with the condensed matter literature. Indeed, several authors—most notably, Dyson himself—also have discussed the structure of the low-temperature series for the spontaneous magnetization beyond order T^4. We make our comparison along four lines of observations.

Our first observation is that all published calculations or estimates of higher-order interaction terms[6,84–86] apparently failed to identify the dominant $T^{9/2}$-correction to the Dyson term in the spontaneous magnetization.

The second observation is that there appears to be consensus in the literature on how graphs related to the *two*-spin-wave problem should manifest themselves beyond T^4. Dyson classified his terms according to the quantity F, where F is the *number of independent particles which are concerned in the interactions which the particular term describes*.[6] For $F = 2$, which is referred to as the *two-spin-wave problem* in Ref. 84, the corresponding corrections are expected to show up at order T^5 according to Refs. 84– 86, hence, these authors seem to agree on that the dominant correction to the Dyson term should be of order T^5 in the spontaneous magnetization. However, this claim is not correct—it is in contradiction with the fully systematic effective field theory analysis which has demonstrated that the dominant correction sets in at order $T^{9/2}$.

The third observation concerns the *three*-spin-wave problem, i.e., the effect of interaction terms with $F = 3$. Dyson identified two such contributions—formulas (128) and (130) in his second article of Ref. 6—and showed that in the spontaneous magnetization these are of order $T^{13/2}$ and T^5, respectively. In the article by Morita and Tanaka,[84] however, it is claimed that the *three*-spin-wave problem starts manifesting itself at order $T^{13/2}$, missing thus the term of order T^5.

Finally, the fourth observation is that the only place in the literature where a Feynman diagram displaying the cateye structure of graph 11c seems to have appeared is in the more recent article by Chang.[85] However, he concludes that interactions originating from such a diagram start showing up only at order $T^{15/2}$ in the spontaneous magnetization. This claim, again, is erroneous, as it contradicts the fully systematic effective theory analysis, which has demonstrated that the leading term originating from a cateye graph is of order $T^{9/2}$.

In view of the quite impressive collection of temperature powers established over the years, one may easily get confused—after all, may some of these temperature powers, again, merely be spurious? One would certainly like to gain some deeper insight into the general structure of the low-temperature series for the spontaneous magnetization beyond the leading correction to the Dyson term. Let us therefore address the problem in a fully systematic way within the effective field theory framework—first on the level of the free energy density.

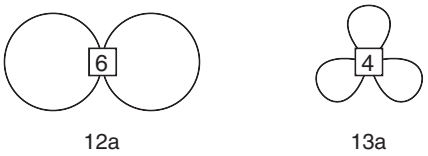

FIG. 4. Two Feynman graphs related to the low-temperature expansion of the partition function for a ferromagnet at order p^{12} and p^{13} in dimension $d = 3 + 1$. The numbers attached to the vertices refer to the piece of the effective Lagrangian they come from. Note that there are further Feynman graphs of order p^{12} and p^{13}, which we have not displayed.

Indeed, it is quite easy to see that corrections due to the spin-wave interaction continue to proceed in steps of $T^{1/2}$. In Fig. 4, we have displayed some of the relevant higher-order graphs, which contribute beyond order p^{11} or, equivalently, beyond $T^{11/2}$. At order T^6 in the free energy density, the two-loop graph 12a with an insertion from $\mathcal{L}^6_{\text{eff}}$ contributes, while at order $T^{13/2}$ the three-loop graph 13a with a vertex from $\mathcal{L}^4_{\text{eff}}$ is relevant.

We may classify the graphs of the effective theory according to the number of loops they contain and discuss the various contributions at the level of the spontaneous magnetization. Interactions related to two-loop diagrams start manifesting themselves through the Dyson term of order T^4 and then proceed in integer steps of T—these are the two-loop graphs with successive insertions from $\mathcal{L}^4_{\text{eff}}, \mathcal{L}^6_{\text{eff}}, \mathcal{L}^8_{\text{eff}}, \ldots$, giving rise to terms of order $T^4, T^5, T^6, \ldots$ in the spontaneous magnetization. Interactions related to three-loop diagrams start showing up at order $T^{9/2}$. They give rise to the dominant correction to Dyson's result, and then also proceed in steps of T—in the effective theory these correspond to the three-loop graphs with successive insertions from $\mathcal{L}^2_{\text{eff}}, \mathcal{L}^4_{\text{eff}}, \mathcal{L}^6_{\text{eff}}, \ldots$, leading to half-integer powers of the temperature: $T^{9/2}, T^{11/2}, T^{13/2}, \ldots$ Four-loop interactions are expected to enter the game at order T^6. They will continue contributing to the spontaneous magnetization in ascending powers of T through terms of order $T^6, T^7, T^8, \ldots$

Accordingly, the low-temperature expansion for the spontaneous magnetization of the ideal ferromagnet exhibits the following general structure:

$$\frac{\Sigma(T)}{\Sigma} = 1 - \alpha_0 T^{\frac{3}{2}} - \alpha_1 T^{\frac{5}{2}} - \alpha_2 T^{\frac{7}{2}} - \alpha_3 \mathbf{T^4} - \alpha_4 \mathbf{T^{\frac{9}{2}}} - \alpha_5 \mathbf{T^5} - \alpha_6 \mathbf{T^{\frac{11}{2}}} + \mathcal{O}(\mathbf{T^6}). \quad (6.4)$$

Note that we have highlighted all terms that are related to the spin-wave interaction. We thus realize that the various published temperature powers as such are not in contradiction with the effective field theory prediction—sooner or later, the effective expansion will hit them all. The point is, however, that there are two gaps in the multitude of published temperature powers—interaction terms of order $T^{9/2}$ and $T^{11/2}$, to the best of our knowledge, have never been identified.

One may say that the effect of the spin-wave interaction on the low-temperature series for the spontaneous magnetization of an ideal ferromagnet is quite peculiar. On the one hand, the interaction starts manifesting itself only at order T^4, i.e., far beyond the Bloch term of order $T^{3/2}$. On the other hand, subsequent interaction corrections closely follow the term of order T^4, starting with $T^{9/2}$ and then proceeding in steps of $T^{1/2}$.

VII. CONCLUSIONS

The question of how the spin-wave interaction manifests itself in the low-temperature expansion of the spontaneous magnetization of an ideal ferromagnet has a long history. Early attempts that ended up with temperature powers of order $T^{7/4}$ and T^2 turned out to be wrong altogether, as shown by Dyson's rigorous analysis, which demonstrated that the spin-wave interaction sets in only at order T^4.

After Dyson's rather complicated analysis, there emerged an active phase of research in which many authors tried to derive the T^4 term in the spontaneous magnetization in a more accessible manner. We also noted in the introductory section that a spurious term of order T^3 in the spontaneous magnetization appeared in those works that were devoted to studying the thermodynamics of ferromagnets in the whole temperature range.

We would like to stress that one of the virtues of the fully systematic effective Lagrangian method is that it is based on symmetry considerations. Indeed, the existence of Dyson's T^4 term—and, at the same time, the absence of a T^3-term—is an immediate consequence of the underlying symmetries inherent in the ideal ferromagnet.

In his collection of selected papers that appeared in 1996,[18] Dyson comments, "After 1966, the subject of spin-wave interactions went into a long sleep." Note that in 1966, Keffer's comprehensive review on spin waves appeared.[35] Still, so it seems, sporadically over time, the peaceful sleep has been interrupted, as several authors were attracted by the problem of what the general structure of the series for the spontaneous magnetization of an ideal ferromagnet beyond the Dyson term should look like. Remarkably, not all of the various findings are consistent with one another. It was our motivation to solve this paradox, making use of the systematic and model-independent method of effective Lagrangians.

As we have demonstrated in the present study, it is rather straightforward to go beyond Dyson's analysis by considering three-loop effects in the effective field theory. Still, the explicit evaluation at order p^{11} is quite nontrivial, as it involves the renormalization and subsequent numerical evaluation of a three-loop graph, which is proportional to an integral over a product of four thermal propagators, each one of them involving an infinite sum. The corresponding interaction term beyond Dyson is completely fixed by the symmetries of the leading-order effective Lagrangian $\mathcal{L}^2_{\text{eff}}$—lattice anisotropies, showing up at higher orders in the effective Lagrangian, do not affect this result. What is quite remarkable is the fact that all previous attempts to go beyond Dyson apparently have failed to correctly identify this interaction term of order $T^{9/2}$ in the spontaneous magnetization of an ideal ferromagnet.

We have also discussed the origin and the structure of even higher-order corrections in the low-temperature expansion of the spontaneous magnetization, pointing out that they continue to proceed in steps of $T^{1/2}$ beyond the contribution of order $T^{9/2}$. Again, earlier attempts to gain insight into the general structure of this series were incorrect.

The present study has thus solved—once and for all—the problem of how the spin-wave interaction in an ideal ferromagnet manifests itself in low-temperature expansion of the spontaneous magnetization beyond the Dyson term.

Hopefully, we have convinced the reader that the effective Lagrangian technique does not merely consist in rederiving known results or in rephrasing condensed matter problems in another language—rather, in many cases as in the present one, it clearly proves to be more powerful than conventional condensed matter methods, allowing one to go to higher orders of the low-temperature expansion in a controlled and systematic manner. In view of the many articles that have dealt with the problem of the manifestation of the spin-wave interaction in an ideal ferromagnet at low temperatures, it is quite striking how efficiently the effective theory analysis settles this question in a conclusive way.

We do not claim to have contributed to the actual experimental situation—spin-wave interactions in a ferromagnet are very weak. Above all, there are many interactions in addition to the exchange interaction in a *real* ferromagnet, which would also have to be accounted for in a more realistic approach. While this would be perfectly feasible within the effective Lagrangian framework, here we have restricted ourselves to the simple model of the *ideal* ferromagnet—after all, it is for this system where corrections to Dyson's result have been derived over the years.

Although there is no such object as a perfectly ideal ferromagnet in nature, still, the "clean" ideal ferromagnet could be investigated in a numerical simulation of the Heisenberg model and the existence of the $T^{9/2}$-term in the low-temperature expansion of the spontaneous magnetization might be verified this way.

ACKNOWLEDGMENTS

I thank Professor Freeman J. Dyson for correspondence and for carefully reading the manuscript. Thanks also to H. Leutwyler and U.-J. Wiese for stimulating discussions and to J. Zittartz for correspondence. Finally, thanks to one of the referees for his valuable remarks on the literature. This work is supported by CONACYT Grant No. 50744-F.

APPENDIX A: EFFECTIVE LAGRANGIAN METHOD

In this appendix we would like to provide the reader not familiar with the effective Lagrangian technique with additional information, hoping that—with the information already given in Secs. II and III A—the paper will become readily accessible to the condensed matter community.

Right at the beginning, we have to emphasize a crucial point regarding the relation between the *underlying* theory and the

effective theory. In the present case of the ferromagnet, the underlying—or microscopic—theory is the Heisenberg model,

$$\mathcal{H}_0 = -J \sum_{n.n.} \vec{S}_m \cdot \vec{S}_n, \quad J = \text{const.}, \tag{A1}$$

which is formulated in terms of the spin operators $\vec{S}$. In the effective field theory, the relevant degrees of freedom are the spin waves, which are described by the spontaneous magnetization (order parameter) vector $\vec{U}$ (see below). We will now elaborate on the fact that **no** explicit equation exists that connects the two rather different objects $\vec{S}$ and $\vec{U}$ appearing in the underlying and the effective theory, respectively.

First, note that the situation is very different from the more conventional approaches to the low-energy physics of a ferromagnet: In Dyson's analysis or in spin-wave theory, e.g., one is faced with the problem to express the spin operators of the Heisenberg model in terms of the bosonic operators, which describe the magnons. This expansion of spin operators in terms of bosonic operators can be done in a variety of ways, e.g., by the Dyson-Maleev or the Holstein-Primakoff transformation. These transformations thus provide an immediate connection between the spin operators of the Heisenberg model and the bosonic magnon operators, which describe the low-energy physics.

The construction of the effective field theory for magnons proceeds in a rather different manner. The only link between the effective and the microscopic theory are the symmetries inherent in the Heisenberg model. These symmetries are inherited by the effective Lagrangian and constrain the construction of the terms in the effective Lagrangian, which is done in a systematic manner. However, within the effective Lagrangian approach, one does **not** pretend to "derive" the effective Lagrangian from the underlying Heisenberg model. There is no equation where the spin operator $\vec{S}$ appears on the left-hand side and the effective field $\vec{U}$ appears on the right-hand side.

Rather, the construction of the effective Lagrangian is based on locality, unitarity, as well as on a symmetry analysis and thus involves a good portion of group theory. The mathematical formalism was developed three decades ago in the context of the strong interaction, where one deals with a spontaneously broken chiral symmetry. The formalism was transferred to condensed matter systems in Ref. 41 and applied to describe spin waves of ferromagnets and antiferromagnets as well as phonons in solids. In these cases, one deals with a spontaneously broken spin rotation symmetry and a spontaneously broken translation symmetry, respectively. In particular, the quite involved group theoretical construction of the leading order effective Lagrangian for the ferromagnet $\mathcal{L}^2_{\text{eff}}$ is presented in detail in that reference, such that here we just focus on some essential aspects.

The effective theory is designed to describe the physics of Goldstone bosons, which are the relevant degrees of freedom at low energies or low temperatures. The Goldstone bosons originate from the spontaneously broken global continuous symmetry, which involves the two groups G and H: While G is the symmetry of the underlying theory, H is the symmetry of the ground state. In the present case of the ferromagnet, the spin-rotation symmetry G = O(3) of the Heisenberg model is spontaneously broken by the ground state of the ferromagnet, which is invariant only under the subgroup H = O(2). The Goldstone bosons in the present case are the spin waves or magnons.

From a group-theoretical point of view, the Goldstone boson fields $U(x)$ live in the coset space G/H. Their transformation properties are fully determined by the structure of G and H. In the present case of the ferromagnet, the spin waves or magnons live in the coset space $O(3)/O(2)$, which may be identified with the sphere S^2. Accordingly, the magnon field may be parameterized by a unit vector $\vec{U}(x)$. The low-energy physics of the ferromagnet can be completely described in terms of the field $\vec{U}(x)$, which represents the direction of the local spontaneous magnetization—the order parameter of the spontaneously broken spin rotation symmetry.

The number of real Goldstone bosons fields n_{GB}, according to the Goldstone theorem,[73–77] is given by the difference of the number of symmetry generators we have in the two groups G and H: n_{GB} = dim(G) − dim(H). In the present case of the ferromagnet, we thus have two real spin-wave fields, which we denote by $U^1(x)$ and $U^2(x)$ or, collectively, by $U^a(x)$ with $a = 1,2$. These spin-wave fields are the basic degrees of freedom in our effective theory and correspond to the fluctuations of the spontaneous magnetization vector $\vec{U} = U^i = (U^1, U^2, U^3)$, which is normalized to one, $|\vec{U}| = 1$. In our convention, the spontaneous magnetization points along the third axis, such that the ground state of the ferromagnet is characterized by $\vec{U}_0 = (0,0,1)$. The two real spin-waves fields, collected in the transverse directions U^1 U^2, represent the fluctuations of the spontaneous magnetization vector $\vec{U}$ around the ground state.

Now that we have identified the basic degrees of freedom of the effective theory—the two real spin-wave fields contained in the magnetization vector $\vec{U}$—we want to systematically construct the terms appearing in the effective Lagrangian. The idea is simple: One writes down in a systematic manner all terms which are invariant under the symmetries that have been identified in the underlying Heisenberg model. The various pieces in the effective Lagrangian can be organized according to the number of space and time derivatives they contain. Since we want to describe the spin-wave physics at low energies, terms in the effective Lagrangian that contain only a few derivatives are the dominant ones, while terms with more derivatives are suppressed. This is what we mean by systematic: organizing the terms in the effective Lagrangian according to the number of derivatives (or magnetic fields, see below) they contain.

Now, in nonrelativistic systems we have to distinguish between space and time derivatives. Since in our analysis we assume space rotation symmetry (the justification was given at the end of Sec. II.), there are no terms with an odd number of space derivatives in the effective Lagrangian. In fact, as derived in detail in Ref. 41, the leading order effective Lagrangian contains a term with one time (∂_0) and a term with two space ($\partial_r \partial_r$) derivatives, as well as a term that involves the magnetic field H and contains no derivative:

$$\mathcal{L}^2_{\text{eff}} = \Sigma \frac{\epsilon_{ab} \partial_0 U^a U^b}{1 + U^3} + \Sigma \mu H U^3 - \frac{1}{2} F^2 \partial_r U^i \partial_r U^i. \tag{A2}$$

It is important to note that, according to this equation, in the systematic counting of derivatives, **one** time derivative (or **one** insertion of the magnetic field) are thus on the same footing as **two** space derivatives—they all are of order p^2 in the derivative expansion of the effective Lagrangian.

The effective action defined by the effective Lagrangian through

$$\mathcal{S}_{\rm eff} = \int d^4x \mathcal{L}_{\rm eff} \tag{A3}$$

is invariant under the spin rotation symmetry O(3), under parity as well as time reversal symmetry—it respects all the symmetries inherent in the Heisenberg model and represents the most general expression of order p^2 involving the spin-wave fields in $\vec{U} = U^i$ one can write down.

The effective Lagrangian of the ferromagnet, in fact, is a rather peculiar object: it is invariant under time-reversal and under O(3) spin rotations only up to a total derivative (see Ref. 41). The effective action, however, is perfectly invariant under these symmetries, as well as under all other symmetries that have been identified in the underlying Heisenberg model.

While the derivative structure of these terms is rigorously determined by the symmetries of the Heisenberg model (again, the detailed and rather involved group-theoretical construction is presented in Ref. 41 and will not be repeated here), each term comes with an effective constant which is not fixed by symmetry. At leading order, we have two such constants, the spontaneous magnetization Σ and the quantity F. The actual values of effective constants in general may be obtained from experiment, from numerical simulation, or, in some cases, from a direct matching of physical quantities calculated both within the effective and the underlying theory framework.

In order to see that this leading-order effective Lagrangian correctly describes the low-energy physics of the ferromagnet, we may derive the corresponding equation of motion, which takes the form[41]

$$\begin{aligned} &\partial_0 U^a + \varepsilon_{ajk} f_0^j U^k + \gamma \varepsilon_{ajk} \Delta U^j U^k = 0, \\ &f_0^j = \mu H \delta_3^j, \quad \gamma \equiv \frac{F^2}{\Sigma}. \end{aligned} \tag{A4}$$

Indeed, this is the familiar Landau-Lifshitz equation, which describes the dynamics of ferromagnetic spin waves.[87] The corresponding dispersion relation amounts to

$$\omega(\vec{k}) = \gamma \vec{k}^2 + \mathcal{O}(|\vec{k}|^4), \tag{A5}$$

taking the familiar quadratic form, characteristic of ferromagnetic spin waves.

It is important to note that, according to the nonrelativistic Goldstone theorem,[73–77] there only exists one type of spin-wave excitation—or one magnon particle—in the low-energy spectrum of the ferromagnet. Indeed, the two real fields $U^1(x)$ and $U^2(x)$ may be combined into one complex field,

$$u = U^1 + iU^2, \tag{A6}$$

which describes the physical ferromagnetic magnon.

We now turn to a more detailed discussion of the Feynman diagrams, which occur in the evaluation of the partition function. The basic formula from which one derives the Feynman diagrams is given by the path integral representation of the partition function[80–82]

$$\mathrm{Tr}[\exp(-\mathcal{H}/T)] = \int [dU] \exp\left(- \int_{\mathcal{T}} d^4x \mathcal{L}_{\rm eff} \right). \tag{A7}$$

The integration extends over all magnon field configurations that are periodic in the Euclidean time direction $U(\vec{x},x_4 + \beta) = U(\vec{x},x_4)$, with $\beta \equiv 1/T$.

In order to derive this basic formula, we start with the functional integral representation of the time evolution operator

$$\langle U'' | \exp(-i\tau\mathcal{H}|U'\rangle = \int [dU] \exp\left(i \int d^4x \mathcal{L}_{\rm eff} \right). \tag{A8}$$

The integration extends over all field configurations $U(\vec{x},t)$, interpolating between $U(\vec{x},0) = U'(\vec{x})$ and $U(\vec{x},\tau) = U''(\vec{x})$. To obtain the analogous integral representation of the operator $\exp(-\tau\mathcal{H})$, one replaces the phase factor $\exp(i\mathcal{S})$ with $\exp(-\tilde{\mathcal{S}})$, where $\tilde{\mathcal{S}}$ is the effective action in Euclidean space,

$$\langle U'' | \exp(-\tau\mathcal{H})|U'\rangle = \int [dU] \exp\left(- \int d^4x \tilde{\mathcal{L}}_{\rm eff} \right). \tag{A9}$$

The integration extends over the same field configurations as in Eq. (A8). In order to obtain the Euclidean effective Lagrangian from $-\mathcal{L}_{\rm eff}$, one merely replaces the Minkowski space metric $g_{\mu\nu} = (+---)$ by $-\delta_{\mu\nu}$.

Finally, to arrive at the trace of $\exp(-\mathcal{H}/T)$, one takes a time interval of length $1/T$, identifies U'' with U', and integrates over U'. The functional integral then extends over all fields that are periodic in x_4 and takes the form displayed in Eq. (A7).

Temperature thus produces remarkably little change: to obtain the partition function, one simply restricts the manifold on which the Goldstone boson fields are living to a torus. The effective Lagrangian remains unaffected—in particular, the effective coupling constants are temperature independent. Here, the essential point is that the boundary conditions in the Euclidean time direction x_4 are dictated by the trace that defines the partition function.

The quantity $\mathcal{L}_{\rm eff}$ on the right hand side of Eq. (A7) is the Euclidean form of the effective Lagrangian, which consists of a string of terms:

$$\mathcal{L}_{\rm eff} = \mathcal{L}_{\rm eff}^2 + \mathcal{L}_{\rm eff}^4 + \mathcal{L}_{\rm eff}^6 + \mathcal{L}_{\rm eff}^8 + \mathcal{O}(p^{10}), \tag{A10}$$

involving an increasing number of space and time derivatives as well as the magnetic field. As we have argued in Sec. II, in our evaluation of the partition function we have to include terms with up to eight space derivatives.

The virtue of the representation (A7) lies in the fact that it can be evaluated perturbatively. To a given order in the low-energy expansion, only a finite number of Feynman graphs and a finite number of coupling constants contribute. More precisely, the low-temperature expansion of the partition function is obtained by considering the fluctuations of the spontaneous magnetization vector field $\vec{U} = (U^1,U^2,U^3)$

around the ground state $\vec{U}_0 = (0,0,1)$, i.e., by expanding U^3 in powers of the spin-wave fluctuations U^a,

$$U^3 = \sqrt{1 - U^a U^a} = 1 - \tfrac{1}{2} U^a U^a - \tfrac{1}{8} U^a U^a U^b U^b - \cdots. \tag{A11}$$

Inserting this expansion into formula (A7), one then generates the Feynman diagrams illustrated in Figs. 1 and 2 of Sec. II. At this point, the reader may find it helpful to also consult Ref. 81—in particular, chapter 3, where the generation of diagrams is discussed. The leading contribution in the exponential of the right-hand side of Eq. (A7) is of order p^2 and originates from $\mathcal{L}^2_{\text{eff}}$. It contains a term quadratic in the spin-wave field U^a—with the appropriate derivatives and the magnetic field displayed in Eq.(A2)—and describes free magnons. The corresponding diagram for the partition function is the one-loop diagram 5 of Fig. 1. Note that in Sec. II we have argued that each loop in a Feynman diagram leads to a suppression of p^3—the one-loop diagram 5 is of order p^5, because it involves two derivatives (p^2) and one loop (p^3).

The remainder of the effective Lagrangian in the path integral formula is treated as a perturbation. The Gaussian integrals are evaluated in the standard manner,[80–82] and one arrives at a set of Feynman rules that differ from the zero-temperature rules of the effective Lagrangian method only in one respect: the periodicity condition imposed on the magnon fields modifies the propagator. At finite temperature, the propagator is given by

$$G(x) = \sum_{n=-\infty}^{\infty} \Delta(\vec{x}, x_4 + n\beta), \tag{A12}$$

where $\Delta(x)$ is the Euclidean propagator at zero temperature,

$$\Delta(x) = \int \frac{dk_4 d^3k}{(2\pi)^4} \frac{e^{i\vec{k}\vec{x} - ik_4 x_4}}{\gamma \vec{k}^2 - ik_4 + \mu H}. \tag{A13}$$

The lines connecting the various vertices occurring in the Feynman diagrams stand for the Euclidean thermal propagator Eq. (A12).

The numbers attached to the vertices in the Feynman diagrams refer to the piece of the effective Lagrangian they come from. Vertices associated with the leading-order effective Lagrangian $\mathcal{L}^2_{\text{eff}}$ we have denoted by a dot. The dot in diagram 10b of Fig. 1, e.g., means that we are considering an insertion from $\mathcal{L}^2_{\text{eff}}$, which contains terms with two space derivatives, terms with one time derivative as well as terms involving the magnetic field and no derivative. Note also that we need all such expressions that involve a total of four magnon fields U^a, as required by the topology of the diagram (four lines connected to the vertex). In the same diagram 10b, we have another vertex that involves the next-to-leading order Lagrangian $\mathcal{L}^4_{\text{eff}}$. Here, all terms involve four space derivatives. As we have argued in Sec. II, terms with time derivatives or terms involving the magnetic field can be eliminated with the equation of motion, such that $\mathcal{L}^4_{\text{eff}}$ takes the simple form given in Eq. (2.6) exhibiting space derivatives only. Moreover, we need all expressions originating from $\mathcal{L}^4_{\text{eff}}$ that contain a total of two magnon fields, according to the topology of the diagram 10b.

In the evaluation of the partition function, throughout this work, we have used the path integral formalism where the quantity $\vec{U}(x)$ is a classical field. Still, the field may be quantized and the Greens function of the magnon particle expressed by bosonic operators via

$$\langle 0|T\{u(\vec{x}, x_4) u^\dagger(\vec{y}, y_4)\}|0\rangle = \frac{2}{\Sigma} \Delta(x - y). \tag{A14}$$

The magnon field operators u and $u^\dagger$ have been constructed in Ref. 43 and are given by

$$\begin{aligned} u(x) &= \sqrt{\frac{2}{\Sigma}} \int \frac{d^3k}{(2\pi)^3} a(\vec{k}) e^{-ikx}, \\ u(x)^\dagger &= \sqrt{\frac{2}{\Sigma}} \int \frac{d^3k}{(2\pi)^3} a(\vec{k})^\dagger e^{ikx}. \end{aligned} \tag{A15}$$

Again, the above Greens function corresponds to the propagation of the physical magnon particle, described by the complex operators $u = U^1 + iU^2$ and $u^\dagger = U^1 - iU^2$, respectively. The bosonic operators $a^\dagger$ and a are the creation and annihilation operators of the ferromagnetic magnon.

APPENDIX B: NUMERICAL EVALUATION OF THE CATEYE GRAPH

To numerically evaluate the integral $\bar{J}$ defined in Eq. (4.15), we introduce the dimensionless variables η and ξ,

$$\eta = T x_4, \quad \xi = \frac{1}{2} \sqrt{\frac{T}{\gamma}} |\vec{x}|. \tag{B1}$$

In the integrals over the torus that involve quartic and triple sums—the first two terms in Eq. (4.15)—we first integrate over all three-dimensional space, ending up with one-dimensional integrals in the variable η. For the quartic sum we obtain

$$\begin{aligned} &\int_{\mathcal{T}} d^4x\, \partial_r G^T(x) \partial_r G^T(x) \partial_s G^T(-x) \partial_s G^T(-x) \\ &\quad = \frac{15}{2048\pi^{9/2}\gamma^{13/2}} T^{\frac{11}{2}} \int_{-1/2}^{1/2} d\eta \sum_{n_1 \ldots n_4 = 1}^{\infty} e^{-\sigma(n_1+n_2+n_3+n_4)} \\ &\qquad \times Q(\eta, n_1, n_2, n_3, n_4), \quad Q(\eta, n_1, n_2, n_3, n_4) \\ &\quad = \frac{\left(\frac{1}{\eta+n_1} + \frac{1}{\eta+n_2} + \frac{1}{-\eta+n_3} + \frac{1}{-\eta+n_4}\right)^{-7/2}}{((\eta+n_1)(\eta+n_2)(-\eta+n_3)(-\eta+n_4))^{5/2}}, \end{aligned} \tag{B2}$$

while for the triple sum we get

$$\begin{aligned} &\int_{\mathcal{T}} d^4x\, \partial_r \Delta(x) \partial_r G^T(x) \partial_s G^T(-x) \partial_s G^T(-x) \\ &\quad = \frac{15}{2048\pi^{9/2}\gamma^{13/2}} T^{\frac{11}{2}} \int_{0}^{1/2} d\eta \sum_{n_2 \ldots n_4 = 1}^{\infty} e^{-\sigma(n_2+n_3+n_4)} \\ &\qquad \times Q(\eta, 0, n_2, n_3, n_4), \quad Q(\eta, 0, n_2, n_3, n_4) \\ &\quad = \frac{\left(\frac{1}{\eta} + \frac{1}{\eta+n_2} + \frac{1}{-\eta+n_3} + \frac{1}{-\eta+n_4}\right)^{-7/2}}{(\eta(\eta+n_2)(-\eta+n_3)(-\eta+n_4))^{5/2}}, \end{aligned} \tag{B3}$$

with

$$\sigma \equiv \frac{\mu H}{T}, \quad \gamma \equiv \frac{F^2}{\Sigma}. \tag{B4}$$

Note that for the triple sums the integration over η only extends over the interval $[0,\frac{1}{2}]$, due to the Θ function contained in the zero-temperature propagator $\Delta(x)$.

The quantities $Q(\eta,n_1,n_2,n_3,n_4)$ and $Q(\eta,0,n_2,n_3,n_4)$ depend in a nontrivial manner on the summation variables. The slowest convergence for the entire expressions Eq. (B2) and Eq. (B3) is observed for the case $\sigma = 0$, where no exponential damping occurs. We have performed the numerical summation in a "Cartesian" way. We first define the vector $\vec{N}_i = (n_1,n_2,n_2,n_4)$. The first partial sum S_1 in the quartic series simply corresponds to the combination $\vec{N}_1 = (1,1,1,1)$ of indices. The second partial sum S_2 then contains all combinations of indices in the vector $\vec{N}_2$ with at least one index equal to two: $(2,1,1,1),\ldots,(2,2,2,2)$, etc. For large values of i and for $\sigma = 0$, the partial sums S_i converge according to $1/{S_i}^{5/2}$. Proceeding in an analogous manner for the triple sums, one obtains the same asymptotic behavior.

Expressions suitable for the numerical evaluation of the remaining three integrals of Eq. (4.15) involving double sums are

$$\begin{aligned}
&\int_{\mathcal{T}\setminus\mathcal{S}} d^4x\,\partial_r\Delta(x)\partial_r\Delta(x)\partial_s G^T(-x)\partial_s G^T(-x)\\
&\quad = \frac{1}{128\pi^5\gamma^{13/2}} T^{\frac{11}{2}} \int_0^S d\eta \int_{\sqrt{S^2-\eta^2}}^{\infty} d\xi\,\xi^6\\
&\qquad \times \sum_{n_1,n_2=1}^{\infty} e^{-\sigma(n_1+n_2)}\, P(\xi,\eta,n_1,n_2),\\
&P(\xi,\eta,n_1,n_2) = \frac{e^{-\xi^2\left(\frac{2}{\eta}+\frac{1}{-\eta+n_1}+\frac{1}{-\eta+n_2}\right)}}{\{\eta^2(-\eta+n_1)(-\eta+n_2)\}^{5/2}},
\end{aligned} \tag{B5}$$

$$\begin{aligned}
&\int_{\mathcal{S}} d^4x\,\partial_r\Delta(x)\partial_r\Delta(x) Q_{ss}(x)\\
&\quad = \frac{1}{128\pi^5\gamma^{13/2}} T^{\frac{11}{2}} \int_0^S d\eta \int_0^{\sqrt{S^2-\eta^2}} d\xi\,\xi^6\\
&\qquad \times \sum_{n_1,n_2=1}^{\infty} e^{-\sigma(n_1+n_2+2\eta)}\, Q(\xi,\eta,n_1,n_2,\sigma),
\end{aligned} \tag{B6}$$

with

$$\begin{aligned}
Q(\xi,\eta,n_1,n_2,\sigma) &= e^{-\xi^2\left(\frac{2}{\eta}+\frac{1}{-\eta+n_1}+\frac{1}{-\eta+n_2}\right)}\\
&\quad \times \frac{\frac{e^{2\eta\sigma}}{\{(-\eta+n_1)(-\eta+n_2)\}^{5/2}} - \frac{e^{\xi^2\left(\frac{1}{-\eta+n_1}+\frac{1}{-\eta+n_2}\right)}}{n_1^{5/2}n_2^{5/2}}}{\eta^5},
\end{aligned} \tag{B7}$$

and, finally,

$$\begin{aligned}
&\int_{\mathcal{R}\setminus\mathcal{S}} d^4x\,\partial_r\Delta(x)\partial_r\Delta(x)\partial_{s\alpha}G^T(-x)|_{x=0}x^\alpha\\
&\quad \times \partial_{s\beta}G^T(-x)|_{x=0}x^\beta = \frac{1}{128\pi^5\gamma^{13/2}} T^{\frac{11}{2}} \int_S^\infty d\eta \int_0^\infty d\xi\,\xi^6\\
&\quad \times \sum_{n_1,n_2=1}^{\infty} e^{-\sigma(n_1+n_2+2\eta)}\, R(\xi,\eta,n_1,n_2)\\
&\quad + \frac{1}{128\pi^5\gamma^{13/2}} T^{\frac{11}{2}} \int_0^S d\eta \int_{\sqrt{S^2-\eta^2}}^\infty d\xi\,\xi^6\\
&\quad \times \sum_{n_1,n_2=1}^{\infty} e^{-\sigma(n_1+n_2+2\eta)}\, R(\xi,\eta,n_1,n_2),\\
&R(\xi,\eta,n_1,n_2) = \frac{e^{-2\xi^2/\eta}}{\{\eta^2 n_1 n_2\}^{5/2}}.
\end{aligned} \tag{B8}$$

It is understood that in the above integrals the radius of the sphere is chosen as $S = \frac{1}{2}$. For large values of i and for $\sigma = 0$, the partial sums S_i related to the above three expressions involving double sums also converge according to $1/{S_i}^{5/2}$.

[1] F. Bloch, Z. Phys. **61**, 206 (1930).
[2] H. A. Kramers, Commun. Kamerlingh. Onnes. Lab. Univ. Leiden. Suppl. **22**, 83 (1936).
[3] W. Opechowski, Physica (Amsterdam) **4**, 715 (1937).
[4] M. R. Schafroth, Proc. Phys. Soc. London A **67**, 33 (1954).
[5] J. van Kranendonk, Physica (Amsterdam) **21**, 81 (1955); **21**, 749 (1955); **21**, 925 (1955).
[6] F. J. Dyson, Phys. Rev. **102**, 1217 (1956); **102**, 1230 (1956).
[7] T. Morita, Prog. Theor. Phys. **20**, 614 (1958).
[8] T. Oguchi, Phys. Rev. **117**, 117 (1960).
[9] F. Keffer and R. Loudon, J. Appl. Phys. (Suppl.) **32**, 2S (1961).
[10] J. Szaniecki, Acta Phys. Polon. **20**, 983 (1961).
[11] J. Zittartz, Z. Phys. **184**, 506 (1965).
[12] D. C. Wallace, Phys. Rev. **153**, 547 (1967).
[13] V. G. Vaks, A. I. Larkin, and S. A. Pikin, Sov. Phys. JETP **26**, 188 (1968).
[14] J. F. Cooke and H. H. Hahn, Phys. Rev. B **1**, 1243 (1970).
[15] J. Szaniecki, J. Phys. C **7**, 4113 (1974).
[16] D. H. Yang and Y. Wang, Phys. Rev. B **12**, 1057 (1975).
[17] E. Rastelli and P. A. Lindgard, J. Phys. C **12**, 1899 (1979).
[18] F. Dyson, *Selected Papers of Freeman Dyson with Commentary* (American Mathematical Society, 1996).
[19] I. Mannari, Prog. Theor. Phys. **19**, 201 (1958).
[20] R. Brout and H. Haken, Bull. Am. Phys. Soc. **5**, 148 (1960).
[21] F. Englert, Phys. Rev. Lett. **5**, 102 (1960).
[22] D. N. Zubarev, Sov. Phys. Usp. **3**, 320 (1960).
[23] R. A. Tahir-Kheli and D. ter Haar, Phys. Rev. **127**, 88 (1962).
[24] R. A. Tahir-Kheli, Phys. Rev. **132**, 689 (1963).
[25] R. B. Stinchcombe, G. Horwitz, F. Englert, and R. Brout, Phys. Rev. **130**, 155 (1963).
[26] H. B. Callen, Phys. Rev. **130**, 890 (1963).
[27] T. Oguchi and A. Honma, J. Appl. Phys. **34**, 1153 (1963).
[28] A. Kühnel, J. Phys. C **2**, 711 (1969).
[29] R. A. Tahir-Kheli, Phys. Rev. B **1**, 3163 (1970).
[30] M. D. Coutinho Filho and I. P. Fittipaldi, Phys. Rev. B **7**, 4941 (1973).

[31] A. Kumar and A. K. Gupta, Phys. Rev. B **28**, 3968 (1983).
[32] R. A. Tahir-Kheli and D. ter Haar, Phys. Rev. **127**, 95 (1962).
[33] I. Ortenburger, Phys. Rev. **136**, A1374 (1964).
[34] T. Morita and T. Tanaka, Phys. Rev. **137**, A648 (1965); **138**, A1403 (1965).
[35] F. Keffer, "Spin Waves," in *Encyclopedia of Physics—Ferromagnetism*, edited by S. Flügge and H. P. J. Wijn (Springer, Berlin, 1966), Vol. 18-2, p. 1.
[36] P. D. Loly, J. Can. Phys. **65**, 1272 (1987).
[37] A. Czachor and A. Holas, Phys. Rev. B **41**, 4674 (1990).
[38] C. P. Hofmann, Phys. Rev. B **65**, 094430 (2002).
[39] S. Weinberg, Physica A **96**, 327 (1979).
[40] J. Gasser and H. Leutwyler, Ann. Phys. (NY) **158**, 142 (1984); Nucl. Phys. B **250**, 465 (1985).
[41] H. Leutwyler, Phys. Rev. D **49**, 3033 (1994).
[42] J. M. Román and J. Soto, Int. J. Mod. Phys. B **13**, 755 (1999).
[43] C. P. Hofmann, Phys. Rev. B **60**, 388 (1999).
[44] J. M. Román and J. Soto, Ann. Phys. **273**, 37 (1999).
[45] P. Hasenfratz and H. Leutwyler, Nucl. Phys. B **343**, 241 (1990).
[46] P. Hasenfratz and F. Niedermayer, Phys. Lett. B **268**, 231 (1991).
[47] P. Hasenfratz and F. Niedermayer, Z. Phys. B **92**, 91 (1993).
[48] W. Bietenholz, Helv. Phys. Acta **66**, 633 (1993).
[49] C. P. Hofmann, Phys. Rev. B **60**, 406 (1999).
[50] C. P. Hofmann, Phys. Rev. B **81**, 014416 (2010).
[51] J. M. Román and J. Soto, Phys. Rev. B **62**, 3300 (2000).
[52] F. Kämpfer, M. Moser, and U.-J. Wiese, Nucl. Phys. B **729**, 317 (2005).
[53] C. Brügger, F. Kämpfer, M. Moser, M. Pepe, and U.-J. Wiese, Phys. Rev. B **74**, 224432 (2006).
[54] C. Brügger, F. Kämpfer, M. Pepe and U.-J. Wiese, Eur. Phys. J. B **53**, 433 (2006).
[55] C. Brügger, C. P. Hofmann, F. Kämpfer, M. Pepe, and U.-J. Wiese, Phys. Rev. B **75**, 014421 (2007).
[56] C. Brügger, C. P. Hofmann, F. Kämpfer, M. Moser, M. Pepe, and U.-J. Wiese, Phys. Rev. B **75**, 214405 (2007).
[57] F.-J. Jiang, F. Kämpfer, C. P. Hofmann, and U.-J. Wiese, Eur. Phys. J. B **69**, 473 (2009).
[58] H. Leutwyler, Helv. Phys. Acta **70**, 275 (1997).
[59] C. P. Burgess, and C. A. Lutken, Phys. Rev. B **57**, 8642 (1998).
[60] D. T. Son, Phys. Rev. Lett. **94**, 175301 (2005).
[61] T. Brauner, Symmetry **2**, 609 (2010).
[62] C. P. Burgess, Annu. Rev. Nucl. Part. Sci. **57**, 329 (2007); Phys. Rept. **330**, 193 (2000).
[63] J. L. Goity, Czech. J. Phys. **51**, B35 (2001).
[64] S. Scherer, Adv. Nucl. Phys. **27**, 277 (2003).
[65] A. V. Manohar, in *Perturbative and Nonperturbative Aspects of Quantum Field Theory*, edited by H. Latal and W. Schweiger (Springer, New York, 1997), p. 311.
[66] H. Leutwyler, in *Hadron Physics 94—Topics on the Structure and Interaction of Hadronic Systems*, edited by V. E. Herscovitz, C. A. Z. Vasconcellos, and E. Ferreira (World Scientific, Singapore, 1995), p. 1.
[67] G. Ecker, Prog. Part. Nucl. Phys. **35**, 1 (1995).
[68] U. Gerber, C. P. Hofmann, F. Kämpfer, and U.-J. Wiese, Phys. Rev. B **81**, 064414 (2010).
[69] U.-J. Wiese and H. P. Ying, Z. Phys. B **93**, 147 (1994).
[70] U. Gerber, C. P. Hofmann, F.-J. Jiang, M. Nyfeler, and U.-J. Wiese, J. Stat. Mech. Theory Exp. (2009) P03021.
[71] F.-J. Jiang and U.-J. Wiese, e-print arXiv:1011.6205.
[72] U. Gerber, C. P. Hofmann, F.-J. Jiang, G. Palma, P. Stebler, and U.-J. Wiese, J. Stat. Mech. Theory Exp. (2011) P06002.
[73] R. V. Lange, Phys. Rev. Lett. **14**, 3 (1965); Phys. Rev. **146**, 301 (1966).
[74] G. S. Guralnik, C. R. Hagen, and T. W. B. Kibble, in *Advances in Particle Physics*, edited by R. L. Cool and R. E. Marshak (Wiley, New York, 1968), Vol. 2, p. 567.
[75] H. B. Nielsen and S. Chadha, Nucl. Phys. B **105**, 445 (1976).
[76] T. Schäfer, D. T. Son, M. A. Stephanov, D. Toublan, and J. J. M. Verbaarschot, Phys. Lett. B **522**, 67 (2001).
[77] T. Brauner, Phys. Rev. D **75**, 105014 (2007).
[78] H. Leutwyler, Ann. Phys. (NY) **235**, 165 (1994).
[79] H. Leutwyler, Nucl. Phys. B, Proc. Suppl. **4**, 248 (1988); in *New Theories in Physics*, Warsaw International Symposium on Elementary Particle Physics, Kazimierz, 1988, edited by Z. Ajduk, S. Pokorski, and A. Trautman (World Scientific, Singapore, 1989), p. 116; also in *Symmetry Violations in Subatomic Physics*, Summer Institute in Theoretical Physics, Kingston, 1988, edited by B. Castel and P. J. O'Donnell (World Scientific, Singapore, 1989), p. 57.
[80] N. P. Landsman and C. G. van Weert, Phys. Rep. **145**, 141 (1987).
[81] J. I. Kapusta, *Finite-Temperature Field Theory* (Cambridge University Press, Cambridge, England 1989).
[82] A. V. Smilga, Phys. Rep. **291**, 1 (1997).
[83] P. Gerber and H. Leutwyler, Nucl. Phys. B **321**, 387 (1989).
[84] T. Morita and T. Tanaka, J. Math. Phys. **6**, 1152 (1965).
[85] C. Chang, Ann. Phys. **293**, 111 (2001).
[86] J. Achleitner, e-print arXiv:1103.1831.
[87] L. D. Landau and E. M. Lifshitz, "Statistical Physics," in *Course of Theoretical Physics*, edited by E. M. Lifshitz and L. P. Pitajewski (Pergamon, London, 1981), Vol. 9, Pt. 2.